Quality of groundwater from domestic wells in the Great Bend Prairie Aquifer, Kansas, USA

by

Brooklyn Armijo

B.S., University of New Mexico, 2020

A THESIS

submitted in partial fulfillment of the requirements for the degree

MASTER OF SCIENCE

Department of Geology
College of Arts and Sciences

KANSAS STATE UNIVERSITY
Manhattan, Kansas

2022

Approved by:

Major Professor
Dr. Matthew Kirk

Copyright

Abstract

The High Plains aquifer supplies nearly one-third of the irrigation water used in the U.S. and drinking water for millions of people, making it a critical groundwater resource. Recent research indicates that nitrate accumulation is degrading groundwater quality in the Great Bend Prairie Aquifer, a portion of the High Plains Aquifer in south-central Kansas. However, little is known about the extent of the problem for domestic (i.e., private) wells, which are used by >30,000 people in the area. To fill this knowledge gap, we collected and geochemically analyzed groundwater samples from 63 domestic wells in the aquifer and combined our results with data collected in 2016 from 23 monitoring wells. We characterized water quality relative to standards for drinking water and used our results in mixing and geospatial calculations to better understand sources of salinity and relationships to land use, respectively. In the private well samples, nitrate as N concentrations averaged 11.2 mg/L as N and exceeded the U.S. Environmental Protection Agency maximum contaminant level for public water supplies (10 mg/L as N) in 28 of 63 samples. Chloride, and sulfate concentrations exceeded the standards in five private water samples. We found that nitrate and uranium concentrations significantly correlate, consistent with studies that have found that nitrate contamination can trigger uranium release from sediments. Using 10 different land use/land cover classes and buffer zones of different radii around each well, we evaluated correlations between nitrate contamination and land use. Primarily, we found negative relationships between the occurrence of nitrate and the urban land use/land cover class. We used a mixing analysis to evaluate the impact on salinity from nearby oil and gas development, evapotranspiration, and natural brine contribution from geological formations underlying the aquifer. Agreeing with previous findings, our results demonstrate that the main contributor of salinity in the aquifer is Permian saltwater, although some data points

show influence from evapotranspiration and contamination from oil and gas brine. We expect that these results will better define the scale of the nitrate contamination and general water quality concerns and their links to land use in the study region.

Table of Contents

List of Figures

List of Tables

Acknowledgements

I want to thank my parents who gave me every opportunity to succeed, and for visiting me as often as you could, I love you guys. I want to thank my brother and sister for answering almost every facetime call and keeping me company during my very lonely first year of grad school. I would also like to thank Walker Vinson, there is just no way I would have been able to do this without you in my corner. For all the times we quarantined together, every trip that we made between MHK and KC (in any weather), and for every type of meal you cooked for me (especially refried beans), thank you.

I would like to thank my graduate advisor, Dr. Matthew Kirk. Your help and knowledge are invaluable. Thank you for the great classes and all the help with my research. I would also like to thank Dr. Kate Zeigler for being an amazing boss and just in general for being you (you are awesome). I want to thank my undergraduate college, the University of New Mexico, for preparing me so well for graduate school. I also want to thank my undergraduate advisor, Dr. Jason Moore, I still think about my undergraduate thesis, and I am still proud very proud of that work.

Chapter 1 - Introduction

The High Plains Aquifer underlies parts of South Dakota, Nebraska, Kansas, Colorado, New Mexico, Oklahoma, and Texas (Figure 1). The Great Bend Prairie Aquifer (GBPA) is part of the High Plains Aquifer limb that extends into the south-central region of Kansas (Figure 1). This aquifer is a vital water resource for south-central Kansas. Although other portions of the High Plains Aquifer are threatened by over pumping, water levels remain stable in the GBPA (Whittemore et al., 2018). However, the sustainability of the aquifer is threatened by water quality. Investigating the water quality further will help us better manage this essential resource.

A recent study on observation wells in the GBPA found that nitrate as N concentrations have increased over the past 40 years (Lane et al., 2020). This study found that out of 22 monitoring wells in the GBPA, seven of them had higher nitrate as N concentrations than the United States Environmental Protection Agency (US EPA) regulations (Lane et al., 2020). The same wells were sampled in another study 30-40 years prior, and only one of them had nitrate as N concentrations that were higher than U. S. EPA regulations (Whittemore, 1993).

The same study found that water quality parameters in the GBPA also depended on the depth of the well and land use at the surface. Lane et al. (2020) found that nitrate concentrations in the shallow aquifer monitoring wells had increased more than the aquifer base samples. They also found that nitrate concentration was higher in cropland monitoring wells than in pasture monitoring wells (Lane et al., 2020). The authors concluded that the bulk of the nitrate contamination was because of surficial additions of ammonium-based fertilizers (Lane et al., 2020). Similar findings were also recorded by Burow et al. (2007) in the San Joaquin Valley, California.

Groundwater quality can also be influenced by subsurface interactions. The GBPA overlies the Dakota Formation in the west and Permian bedrock in the east (Figure 1). There is no indication of the Dakota Formation causing groundwater quality degradation; however, the Permian bedrock contains evaporites and salt cements, which cause the water from this unit to be classified as a brine (Whittemore et al., 1992; Buddemeier, 1994; Townsend and Young, 1995). The Dakota Formation overlies the Permian bedrock in the west and acts as an aquitard (i.e., no mixing can occur between the GBPA and the Permian brine where the Dakota Formation separates them) (Whittemore et al., 1992; Buddemeier, 1994; Townsend and Young, 1995). In the eastern region of the GBPA, the aquifer directly overlies the Permian units, and in these areas, Permian water has been distinguished as a source for salinity increases in GBPA water (Whittemore, 1993). Our spatial comparison of the water quality of wells drilled above the underlying Cretaceous and Permian bedrock units may provide context for water quality differences from the east to the west of the GBPA.

Variability of occurrence and thickness of clay lens and layers in the bedrock can also affect groundwater quality (Townsend and Young, 1995). The occurrence of clay lenses and layers can act as aquitards and limit the downward migration of surficially sourced contaminants (Townsend and Young, 1995). Townsend and Young (1995) found a significant negative correlation between clay lens length and nitrate contamination in Stafford County (a county within the GBPA). The statistical analysis we performed on the occurrence and thickness of clay intervals and nitrate may provide insight into the relationship between nitrate and clay lens length on a broader area of the GBPA.

Although Lane et al. (2020) documented increasing salinity and nitrate concentrations in monitoring wells in the GBPA sampled 30-40 years prior by Whittemore (1993), questions

remain. How many private well owners within the GBPA are drinking water with hazardous levels of nitrate? Is there a correlation between land use/land cover (LULC) and water quality in these wells? Is there an aquifer-wide correlation between clay intervals or bedrock type and groundwater contaminants?

To answer these questions, we collected 63 groundwater samples from private water wells within the GBPA. We utilized data from a 2016 data set from monitoring wells within the GBPA to increase the number of samples analyzed to consider a greater part of the aquifer. We analyzed the aqueous geochemistry of these samples and analyzed correlations among nitrate and bedrock changes and changes in LULC. We also utilized a mixing analysis to better characterize sources of salinity within the aquifer. We completed statistical analysis and created figures of our data using ArcMap 10.8.1, Geochemists Workbench Community Edition 15.0, Microsoft Excel, and GraphPad Prism 9.3.1. The results of our efforts will help us to better understand water quality in private wells in the GBPA and nitrate contamination and its relationship with bedrock and LULC.

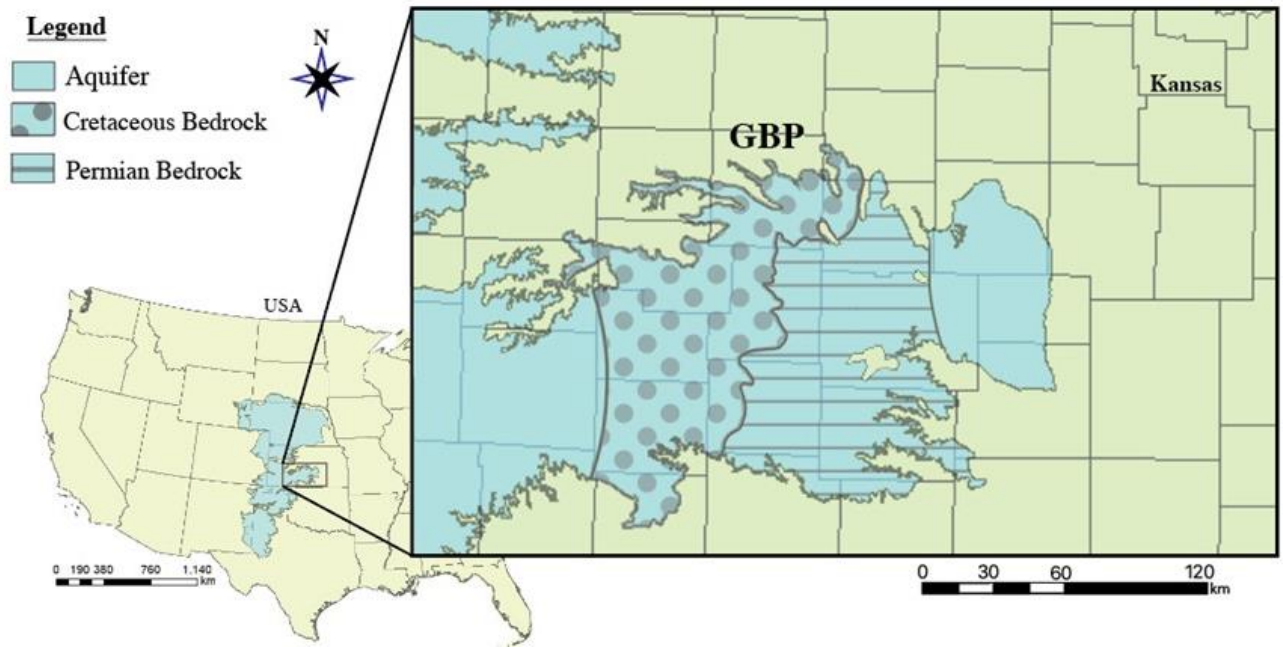

Figure 1. Extent of the Great Bend Prairie Aquifer within the High Plains Aquifer. Associated generalized bedrock geology is shown only within the Great Bend Prairie Aquifer. Base maps modified from KGS (2012) and ESRI (2021).

Chapter 2 - Adverse Effects of Nitrate

The EPA has listed the maximum contaminant level of nitrate as N at 10 (mg/L) for more than one reason (US EPA, 2015). The consumption of contaminated water by infants below the age of six months can cause shortness of breath, Methemoglobinemia (blue baby syndrome), and even death (US EPA, 2015). Nitrate can also cause higher instances of toxic trace elements such as uranium and selenium (Gates et al., 2009; Nolan and Weber, 2015; US EPA, 2015). Uranium is a dangerous toxic trace element because it increases the risk of cancer and has also been linked to noncancerous risks such as kidney toxicity (US EPA, 2015). It is worth noting that in a recent study of the water quality of the GBPA from samples acquired from monitoring wells, trace element contamination was not found (Lane et al., 2020)

Nitrate is also a threat to human (and animal) health because it can be transported in runoff and through groundwater-surface water interactions, eventually leading to accumulation in lakes and ponds (US EPA, 2013, 2015). This nitrate accumulation becomes a source of nutrients for cyanobacteria in harmful algal blooms (US EPA, 2013, 2015). Algal blooms can release cyanotoxins (Chapra et al., 2017). The removal of these toxins is costly and can be only 60% effective (Zamyadi et al., 2012). The physical effects of these toxins when people or animals ingest them (or come into physical contact with them) causes many different symptoms and can lead to death (CDC, 2018). Harmful algal blooms also cause dead zones (anoxic zones) that can kill aquatic life within the range of the anoxic zone (US EPA, 2013).

Chapter 3 - Hydrogeology of the Great Bend Prairie Aquifer

The GBPA is comprised of unconsolidated sediments deposited by the ancestral Arkansas River during the Pliocene and Pleistocene (Fader and Stullken, 1978). This aquifer is made up of interleaved sands, gravels, loess, and lenses of silt and clay (Fader and Stullken, 1978; Whittemore, 1993). The GBPA units overlay Cretaceous bedrock in the west and Permian bedrock in the east (Figure 1) (Whittemore, 1993). There is an erosional contact between the aquifer and the underlying bedrock, such that the sediments of the aquifer have filled in ancient erosional topography, causing the aquifer thickness to vary from 40-150 ft (Fader and Stullken, 1978; Whittemore, 1993). The average saturated thickness reported for Groundwater Management District 5 (the GBPA) is 107 ft (Whittemore et al., 2018).

Cretaceous aged bedrock underlies the aquifer's western half and is primarily composed of the Dakota Formation. The average thickness of the Dakota Formation is 250 ft, and the lithology of the unit in south-central Kansas is highly variable (KGS, 1998). The upper portion of the Dakota contains claystone, fluvial sandstone, estuarine sandstone, and shale (KGS, 1998). The lower portion contains variegated mudstone and lens of claystone, siltstone, sandstone, and conglomerate deposits (KGS, 1998). The dominant composition of the sandstone layers and lens is fine to medium-grained quartz particles (KGS, 1998). The Dakota Formation contains aquitard units, the previously mentioned shale, and this creates an impermeable horizon that inhibits contact between GBPA water and underlying Dakota Aquifer water (Buddemeier, 1994; KGS, 1998). The depositional environment of the Dakota Formation is a coastal plain; however, local changes in environment lead to the lateral variability in facies types (KGS, 1998; Whittemore et al., 2014).

The other half of the GBPA, on the eastern side, overlies Permian bedrock (Figure 1). There is an erosional unconformity between the Permian and Cretaceous units (Figure 2). The Permian currently has 31 distinguishable formations that are formally recognized by the Kansas Geological Survey (West et al., 2010). The total thickness of the Permian bedrock can be greater than 3500 ft (Mudge, M. R. et al., 1967; West et al., 2010). The Permian units contain vast deposits of red beds and evaporites that can have a maximum thickness of 1400 ft (Whittemore, 1993; Buddemeier, 1994; Townsend and Young, 1995; West et al., 2010). During the deposition of these evaporite beds, evaporation exceeded precipitation, and it is likely that some of these deposits are from evaporated seawater (West et al., 2010). The lower Permian units are characterized by limestone, silty limestone, fine sandstone, silty shale, black shale, and mudstone, deposited by transgression and regression of the Panthalassic Ocean (West et al., 2010). The middle Permian units are rich in salt (it has economic worth in some areas with thicknesses >700 ft) and include a red siltstone and a fine silty sandstone, overlain by sandstone and shale, both containing gypsum; above this, there are gypsum and anhydrite beds with thin red mudrocks separating them (West et al., 2010). Throughout these middle units, there are interbedded anhydrite and salt deposits; the sandstones within this subsection are typically arkosic (West et al., 2010). The units were deposited in lagoonal environments with chloride and sulfate flats (West et al., 2010). The upper Permian units are not exposed within the area of the GBPA, they exist in the southwest corner of Kansas (West et al., 2010).

The GBPA and the underlying Permian beds have no lithologic separation, and the freshwater of the GBPA could become mixed with the salty brine, thus causing the groundwater to have higher salinity (increase in concentrations of soluble ions such as, sodium, sulfate, calcium) and degrading water quality (Whittemore, 1993; Buddemeier, 1994; Townsend and

Young, 1995). This is a concern because this aquifer is the primary source of fresh water in this region (Buddemeier, 1994). Unlike the Permian units in the east, the Dakota Formation in the west is largely devoid of evaporite deposits, thus the Dakota Formation inhibits contact between the GBPA (in the western portion) and the underlying Permian evaporites there may be less contamination of Permian brine (because of the aquitard) (Whittemore et al., 1992).

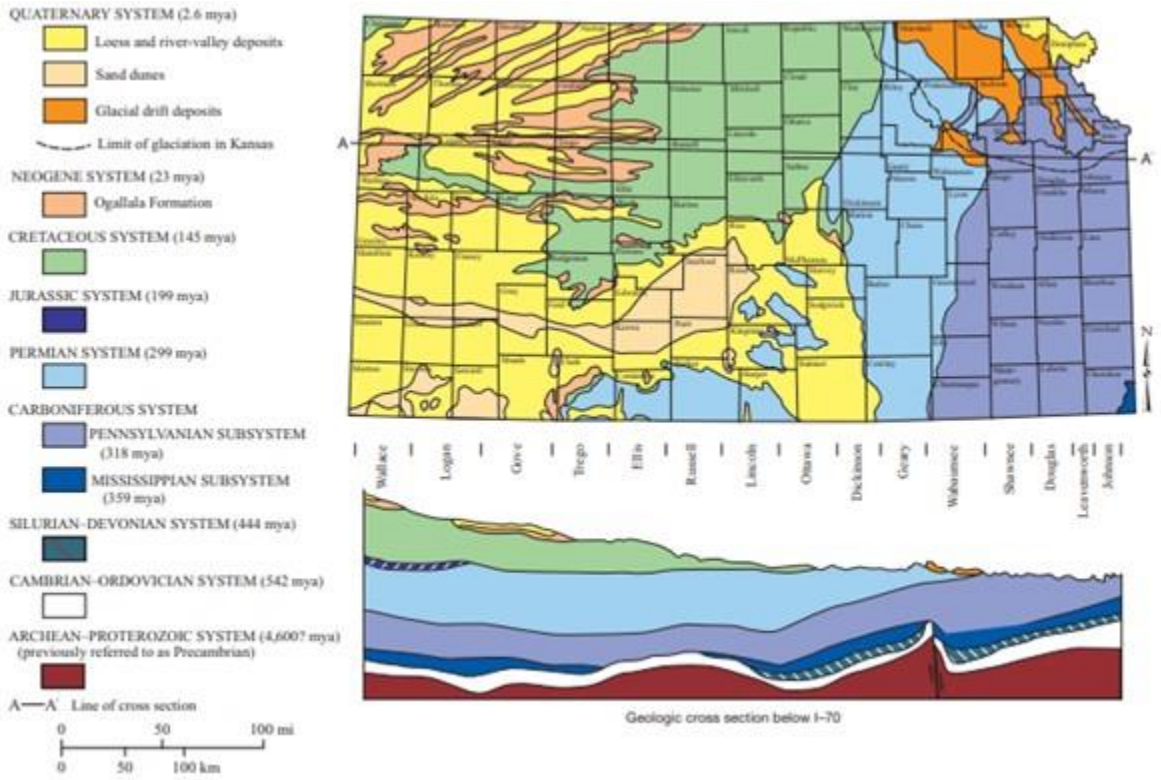

Figure 2. Surficial geologic map and cross section demonstrating the contact and exposure of the Cretaceous and Permian units (West et al., 2010).

Chapter 4 - Methods

Study Area

The study area includes the area north of Interstate 50, and between the towns of Great Bend to the north, Larned to the west, and Hutchinson to the east. In this area the GBPA is between 40-150 ft thick (Fader and Stullken, 1978; Whittemore, 1993). The dominant land use in the Great Bend Prairie area is agriculture. We chose this study area because it was a manageable size for our research group, and within it, most residents primarily use private well water.

Although some portions of the High Plains Aquifer are threatened by over pumping, water levels remain largely stable in the GBPA (Whittemore et al., 2018). However, the sustainability of the aquifer is threatened by water quality degradation. Approximately 130,000 people use the GBPA for drinking water from a public supply system, and 33,000 people obtain their water from private domestic wells (Balleau Groundwater, INC., 2010). The US EPA requires that public water systems be tested to ensure that the water is safe for consumption and free of specific concentrations of contaminants. People who have private domestic wells are not required to test their water; therefore, the 33,000 people could have a water source that does not meet the U. S. EPA's constraints for safe consumption.

The Kansas Environmental Public Health Tracking Program, a branch of the Kansas Department of Health and Environment, reported that there were 26 incidents of public water affected by harmful algal blooms in 2017 (KS-EPHT and KDHE, 2017). In 2021 there were 48 listed advisories on water bodies in the state of Kansas that had harmful algal blooms (Kansas Water Authority, 2022).

Study Design

The original sampling strategy was to collect 25 samples in the western region, underlain by Cretaceous bedrock, and 25 in the eastern part, underlain by Permian bedrock (Figure 1). We identified this as an appropriate target number of wells to analyze trends between bedrock and water quality based on Alley, 1993, who concluded that a sample size below 20 might have too much variability for characterizing regional aquifers. We surpassed our initial goals and sampled 26 wells in the west and 37 wells in the east (Figure 3). Because of the frequency of oil and gas wells (in use, plugged, and abandoned), and landscapes that have the potential to undergo evapotranspiration in the GBPA area, wells were not selected by proximity to oil and gas producing wells or proximity to land with potential for evapotranspiration, this analysis was evaluated using groundwater mixing analysis. Wells were also not selected based upon surrounding LULC; this was evaluated after all water samples were collected. To gain an understanding on the water quality in the area, we considered the following primary and secondary contaminants (which could be anions, cations, or trace elements) set forth by the U. S. EPA shown in Table 1.

List of EPA Contaminants Considered in this Study			
Anions (mg/L)			
Primary Contaminant		Secondary Contaminant	
Fluoride	4	Chloride	250
Nitrate-N	10	Sulfate	250
Nitrite	1		
Cations (mg/L)			
None			
Trace Metals (ppb=µg/L)			
Primary Contaminants (no secondaries present)			
Arsenic	10	Manganese	50
Cadmium	5	Selenium	50
Chromium	100	Uranium	30
Copper	1300	Zinc	5000
Iron	300		

Table 1. List of all U. S. EPA primary and secondary contaminants considered in our study, units are reported in (mg/L) and (µg/L) (US EPA, 2015).

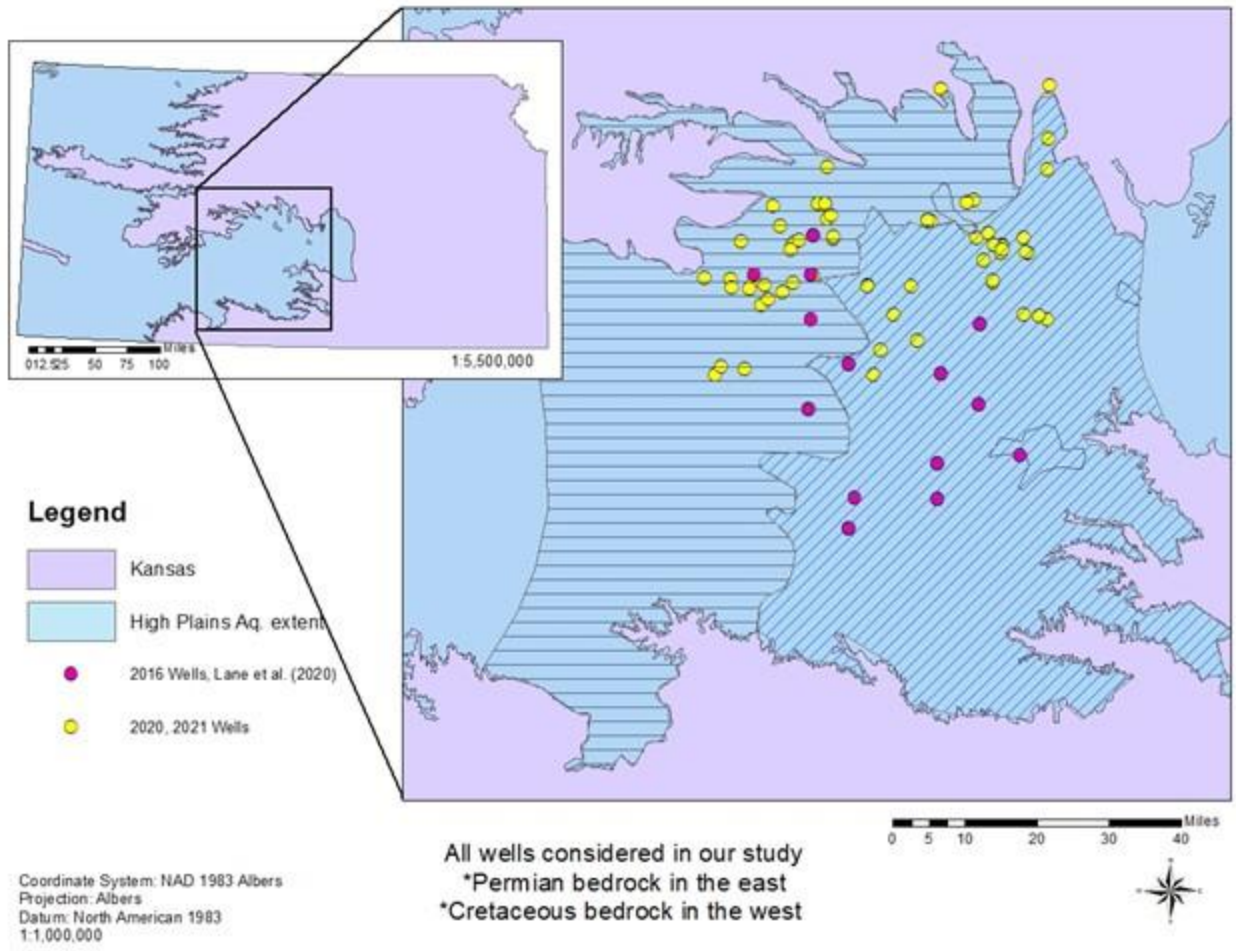

Figure 3. Bedrock map of the Great Bend Prairie Aquifer area, including our 86 well points sampled in 2016 (sampled by Lane et al. 2020), 2020, and 2021. Diagonal blue hatching represents Permian, and the black horizontal lines represent Cretaceous. The 2016 monitoring wells were sampled in couples (Lane et al., 2020). Base maps modified from KGS (2012) and ESRI (2021).

Field Methods

We decided that our research would be a good opportunity for public outreach, and we gave the option to send our water quality analysis results to every well owner that we met with. The well owners were usually more eager to participate after we told them that we could provide this information and that it was going to be free. Many well owners already knew that they were

at risk for nitrate as N contamination, they just had not had their water tested yet. We were able to send the results to each well owner by early October of 2021.

Once a well was identified as a target for sampling, we recorded its latitude and longitude location using the Gaia GPS application set to datum WGS84. We gained access to the well water through outdoor hydrants or spigots on the outside of the resident's home. We ran the spigots and hydrants for a standard ten minutes, which would flush out any stagnant water or recharge water not representative of the aquifer water and leave us with samples directly from the aquifer, before putting the hose tip at the bottom of a 1 L graduated cylinder. Because the hose was pushed to the bottom, the aquifer water ran past the field measurement devices on the way out of the cylinder, which allowed for the least amount of interaction between the sample and the atmosphere. We measured temperature, pH, conductivity, and dissolved oxygen in the field using an Oakton PC 450 to measure pH, conductivity, and temperature. We used a YSI Pro 2030 to measure the dissolved oxygen (in mg/L and percent saturation), conductivity, specific conductance, and temperature again. We recorded measurements every five minutes until three similar measurements were obtained in a row. After the field measurement values had stabilized, we collected samples for analysis of anions, cations, trace elements, dissolved organic carbon, and total nitrogen.

Our field sampling equipment included 0.45 micrometer filters, 30 mL syringes, 30 mL Nalgene sample bottles, and glass amber bottles. We rinsed the syringes thoroughly in lab at Kansas State University with 18 megaohm deionized water. To prepare the plastic Nalgene bottles we soaked them in an acid bath overnight and rinsed with 18 megaohm deionized water. We also soaked the amber bottles in the same acid bath overnight and baked them at 100 degrees Celsius for 12 hours, to remove any C and other ions.

In the field, we used the 0.45 micrometer filter to ensure we were measuring dissolved ions as opposed to particulates. We used the Nalgene bottles for anion and cation sample storage and the glass amber bottles for dissolved organic carbon samples. At each well we obtained a 30 mL sample for cations, anions, and dissolved organic carbon. We stored the water samples in coolers on ice blocks until the end of the sampling day, when we could move them immediately to refrigerators.

Geochemical Analysis

We transported the samples back to the hydrology lab at Kansas State University and preserved the cation samples by acidifying them to a pH of <2 with trace metal grade nitric acid. We also preserved the total nitrogen and dissolved organic carbon samples by acidifying them to a pH of <2 with hydrochloric acid. The anion samples cannot be preserved, but we processed them as quickly as possible after they were collected. We analyzed the samples for alkalinity, cation concentrations, anion concentration, total nitrogen, and total organic carbon. The trace element samples were sent to the University of Nebraska-Lincoln for analysis.

We analyzed the concentrations of the cations and anions using a Dionex ICS-1100 Ion Chromatograph. After charge imbalance calculations were completed using preliminary results from the Dionex ICS-1100, we reran the samples that had <5% charge imbalances. However, some samples had been used in their entirety, and could not be rerun. Even for the samples we could not rerun, there were no charge imbalances greater than 10%.

We evaluated the detection limits of this instrument using US EPA Method 300.1-1. To test the alkalinity of the samples, we performed alkalinity titrations using the Gran alkalinity method, with a burette and 0.02 N sulfuric acid as the titrant. We used the USGS Web-Based Alkalinity Calculator version 2.22 and selected the Gran function plot as our analysis method

(USGS, 2012). Staff members at the Redox Biology Center at the University of Nebraska-Lincoln, used an Inductively Coupled Plasma-Mass Spectrometer (ICP-MS) to analyze our samples for trace elements.

To evaluate the mixing relationships between the GBPA, the underlying Permian bedrock, and oil and gas produced brines, we used bromide and chloride as tracers. Mixing between the GBPA and the brine-containing Permian bedrock has been known to occur, but additions from contaminated water produced in nearby oil fields is also possible (Whittemore, 1993). To observe the mixing trends in our study area we employed the use of mixing curves that use end member water chemistry data to define the water's origin. Plotting these curves with our data gave us a better understanding of the sources of salinity in the GBPA. We used previously defined mixing curves and data points from wells with oil and gas contamination to evaluate the mixing relationships of water in the GBPA, and we also considered the effects of evapotranspiration. Using conservative ions, chloride concentrations, bromide/chloride ratios, and nitrate as N concentrations, we analyzed mixing relationships between recharge water, Permian brine, oil and gas brine, and water affected by evapotranspiration. The presence of nitrate above the GBPA background value (4 mg/L nitrate as N) indicates surficial processes have affected the water (Whittemore, 1993). In this case, it also indicates evapotranspiration. Evapotranspiration, which is also a surficial process, can cause the concentrations of dissolved ions in a fluid to increase because of the removal of fresh water

Geospatial Analysis

There is an abundance of literature on LULC having an influence on surface water quality; however, literature considering correlations between LULC, and groundwater quality is sparse. Typically, studies evaluating correlations between groundwater and LULC will consider an area of land around the focal point of the well sampling point (Liu et al., 2020). Most studies use circular areas (buffer zones) although in study areas with significant run off, the buffer zone may be an entire watershed (Liu et al., 2020). Liu et al. (2020) reported that many groundwater quality and LULC studies use circular 500 m buffer zones, but that size is not appropriate for some study areas due to variances in soil and topography (Liu et al., 2020). Ahn et al. (1999) used relatively small buffer zones (50 m, 100 m, and 150 m) around the aquifer sampling points, Liu et al. (2020) used buffer radii of 500 m to 2500 m, and Huang et al. (2019) (in a surficial water study) considered 500 m, 800 m, 1000 m, 1200 m, 1500 m, and 1800 m. Liu et al. (2020) used a multivariate regression analysis to evaluate the most appropriate buffer zone size specifically for nitrate as N and total N, they concluded that the 1000 m was the optimal radius for nitrate as N and LULC correlations. Because of the variability in buffer sizes in the literature, for our study we decided to use a broad range of sizes to investigate trends between nitrate as N and LULC near to the well, and far from the well.

It is important to understand relationships between LULC and groundwater quality parameters, therefore we decided to complete a geospatial analysis to better understand trends between LULC and the presence of nitrate as N (Whittemore, 1993). Also included in our geospatial analysis are trends between nitrate as N and bedrock changes. The bedrock changes from east to west, such that we can pinpoint on a map which bedrock type each well is drilled above (Figure 3). We obtained LULC maps from the Kansas Biological Survey's website, where

the most recent data they had was from 2015. We selected the 2015 Kansas Land Cover Patterns L1 map which has an estimated overall accuracy of 81% (Peterson and Egbert, 2017). Kansas Biological Survey created the land cover satellite imagery and data from Landsat 8 and MODIS (Peterson and Egbert, 2017). We completed our spatial analysis using ArcMap 10.8.1 and the data downloaded from the Kansas Biological Survey's website.

We projected the LULC map in NAD Albers 1983, an equal area projection. This projection preserved the areas of the LULC polygons, which was the best option for our data because we require accurate area dimensions for our analysis (i.e., areas not stretched or altered by cartographic projection). We projected the buffer zone maps in an equal area projection as well (Figure 4).

We input an excel spreadsheet with each well's attribute information (including the well name, latitude, longitude, and associated geochemistry) and the LULC raster data set from the KBS website, into ArcMap. We used the following tools in ArcMap, Raster to Polygon, Buffer analysis, Intersect, Calculate Geometry, Field Calculator, and Table to Excel. We created 100 m, 200 m, 500 m, 800 m, 1000 m, 1200 m, 1500 m, 2500 m, and 3000 m buffer zones around each well point. Using the Intersect tool, we input the buffer zones and the LULC polygon layer. The Intersect tool acts like a cookie-cutter and our products from this step were buffer zones that contained the LULC polygons at the set buffer size (Figure 4).

To calculate the percentage of LULC in each buffer zone, we used the total area of the buffer zone, and the total area of the LULC types present. We used the tool Field Calculator to divide the area of the LULC types over the total area of the buffer zone and multiplied them by 100 to get the percent of LULC per buffer area. We repeated this step for each buffer zone size. We input the percentages into Excel and used the Pivot Table function to add up the percentages

for each buffer zone around each well using the well's label as a basis of addition. There are limitations to this type of analysis. The water in the GBPA flows to the east, and water that recharges from the surface may have flowed from the west, and therefore may not be representative of the land use directly above the well it was pumped from.

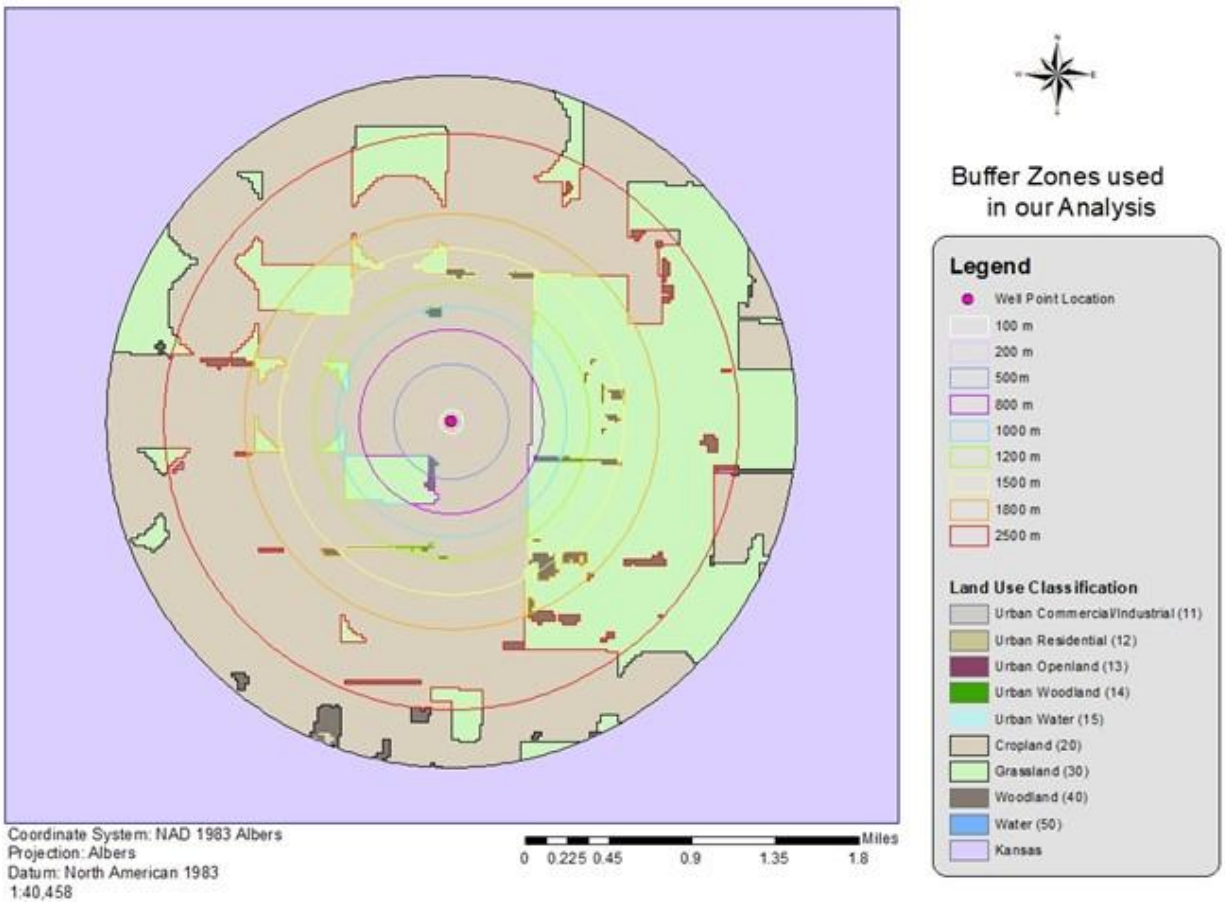

Figure 4. Buffer zones of different radii around an example well point with associated land use/land cover included. Base maps modified from KGS (2012), ESRI (2021), and Peterson and Egbert (2017).

Well Construction Data

We obtained well depth, well screen depth, and clay lens data for as many wells as possible using the Kansas Geological Survey's (KGS) Kansas Water Wells Interactive Map (Figure 5). This interactive map has an exhaustive list of almost every water well (private or monitoring) in the state of Kansas. Within the platform we used each sampling points' latitude and longitude location in the Go To menu option to locate the wells. If the well log data had been digitized by the KGS, we could then click on the well point in the map and obtain the well log. Using this method, we were able to find well logs for 47 of the 63 private wells. In the well logs we found well depth, screen interval, and clay lens occurrence data. Unfortunately, some of the well logs did not include the lithologic log or the depth and interval of the well screen, this decreased our sample size in any analysis considering these parameters. Some of the well owners had their well information and were able to provide us with reliable depth measurements, this was the case for three of the 63 private wells.

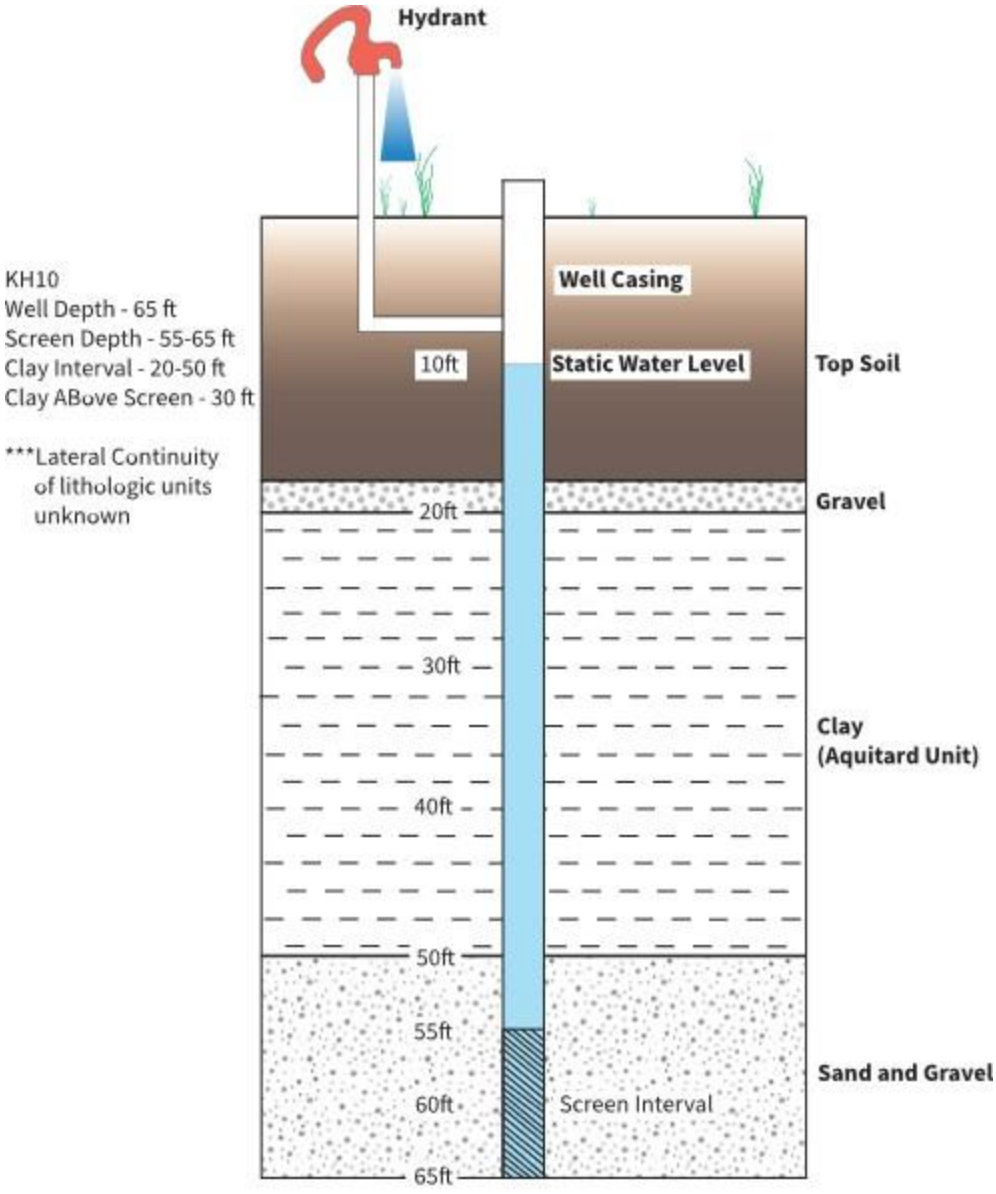

Figure 5. This is an example of the data we collected from well logs using sample, KH10. Included in the figure is the well depth, screen depth and interval, and depth and interval of clay lens (KGS, 2022a).

Statistical Analysis

We used GraphPad Prism 9.3.1 to complete the statistical analysis of our results. We evaluated statistical analysis between nitrate as N and LULC percentages for each buffer zone, trace element concentrations, well depth, clay lens length above screen depth, field

measurements, and ion concentrations. We chose the non-parametric Spearman Rank test because it considers negative and positive correlations between two parameters. This analysis yields two values, an r value (Spearman's rank coefficient value) and a P value (statistical significance value). To evaluate statistical significance between chloride concentrations and bedrock, we chose the Mann-Whitney Test, which also yields a P value.

Chapter 5 - Results

Groundwater Geochemistry

The results from the analysis of field measurements, alkalinity titrations, cation concentrations, and anion concentrations are shown below in Table 2. The temperature averaged 17.57°C. pH remained near to the range of 7 and averaged 7.27. Alkalinity concentrations, in mg/L calcium carbonate, averaged 224. The concentrations for dissolved anions, fluoride, chloride, bromide, sulfate, and nitrate, averaged (in mg/L) 0.41, 355.3, 0.2, 89.42, 10.62, respectively. Concentrations for dissolved cations, sodium, potassium, magnesium, calcium, and strontium, averaged (in mg/L) 224.7, 7.96, 14.79, 105.5, and 4.25, respectively.

The US EPA has a set Maximum Contaminant Level (MCL) for each identified contaminant, Table 1 describes the primary and secondary MCL's considered in our study (US EPA, 2015). Concentrations for some of the parameters exceed primary or secondary MCL's for the data set as a whole, 14 samples had chloride concentrations that were higher than the US EPA secondary MCL of 250 mg/L, and seven samples had higher sulfate concentrations than the secondary MCL of 250 mg/L (US EPA, 2015). We found the primary contaminant nitrate as N to be higher than the MCL of 10 mg/L as N in 35 of the 86 samples, the spatial distribution of these wells is shown in Figure 6 (US EPA, 2015).

Results from the trace element analysis are shown in Figure 7. In our trace element analysis for the data set as a whole, one sample had concentrations above the secondary MCL for manganese, 500 ppb, one sample had concentrations above the secondary MCL for iron, 300 ppb, and one sample had concentrations higher than the primary MCL for uranium, 30 ppb (US EPA, 2015).

Parameter	Number of Values	Minimum	Mean	Maximum
T (°C)	85	14.3	17.57	27.1
pH	86	6.78	7.27	7.75
C (uS/cm)	71	331	1768	36900
DO (mg/L)	59	0.1	3.75	9.2
Alk mg/L CaCO3	86	103.6	224	339.9
F- (mg/L)	85	0.05	0.41	1.26
Cl- (mg/L)	86	3.02	355.3	12958
Br- (mg/L)	75	0.06	0.2	0.92
SO4 2 - (mg/L)	86	5.22	89.42	1275
Na+ (mg/L)	86	9.06	224.7	7817
K+ (mg/L)	86	1	7.96	123.8
Mg2+ (mg/L)	86	2.99	14.79	163.8
Ca2+ (mg/L)	86	14.1	105.5	525.2
Sr2+ (mg/L)	81	1	4.25	37.2
NO3-N (mg/L)	86	0.06	10.62	52.3
Well depth (ft)	73	26	81.86	175
Clay above screen	31	2	26.87	66

Table 2. Minimum, mean, and maximum values of anions, cations, and field measurements. T=Temperature, C=Conductivity, DO=Dissolved Oxygen, Alk=Alkalinity.

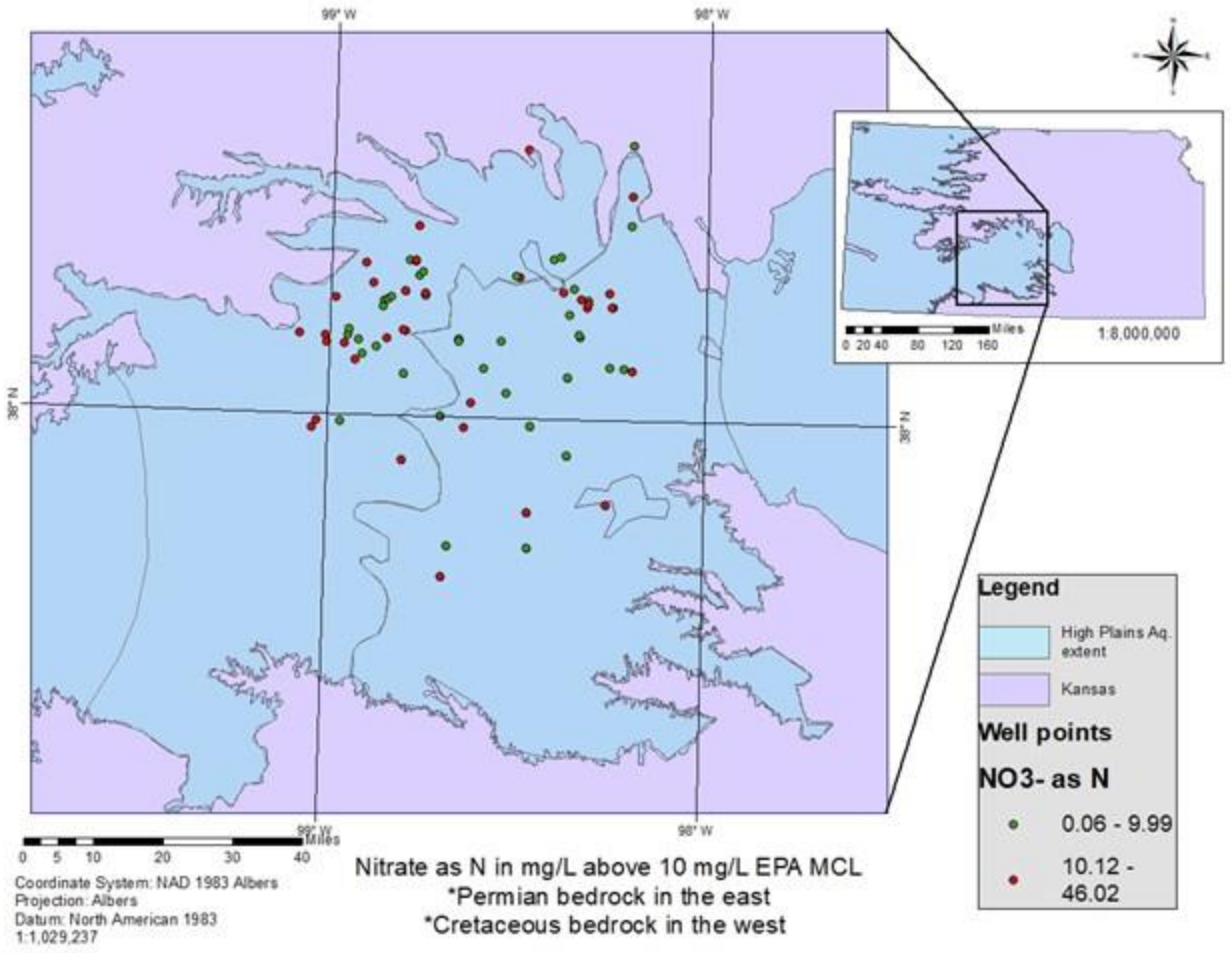

Figure 6. Spatial distribution of data points including our 86 well points sampled in 2016 by Lane et al. (2020), 2020, and 2021. We color coded wells with greater than the MCL of nitrate as N (10 mg/L) in red, and non-contaminated wells are in green (US EPA, 2015). Contaminated wells were distributed evenly throughout the central region of the GBPA. Map modified from KGS (2012), and ESRI (2021).

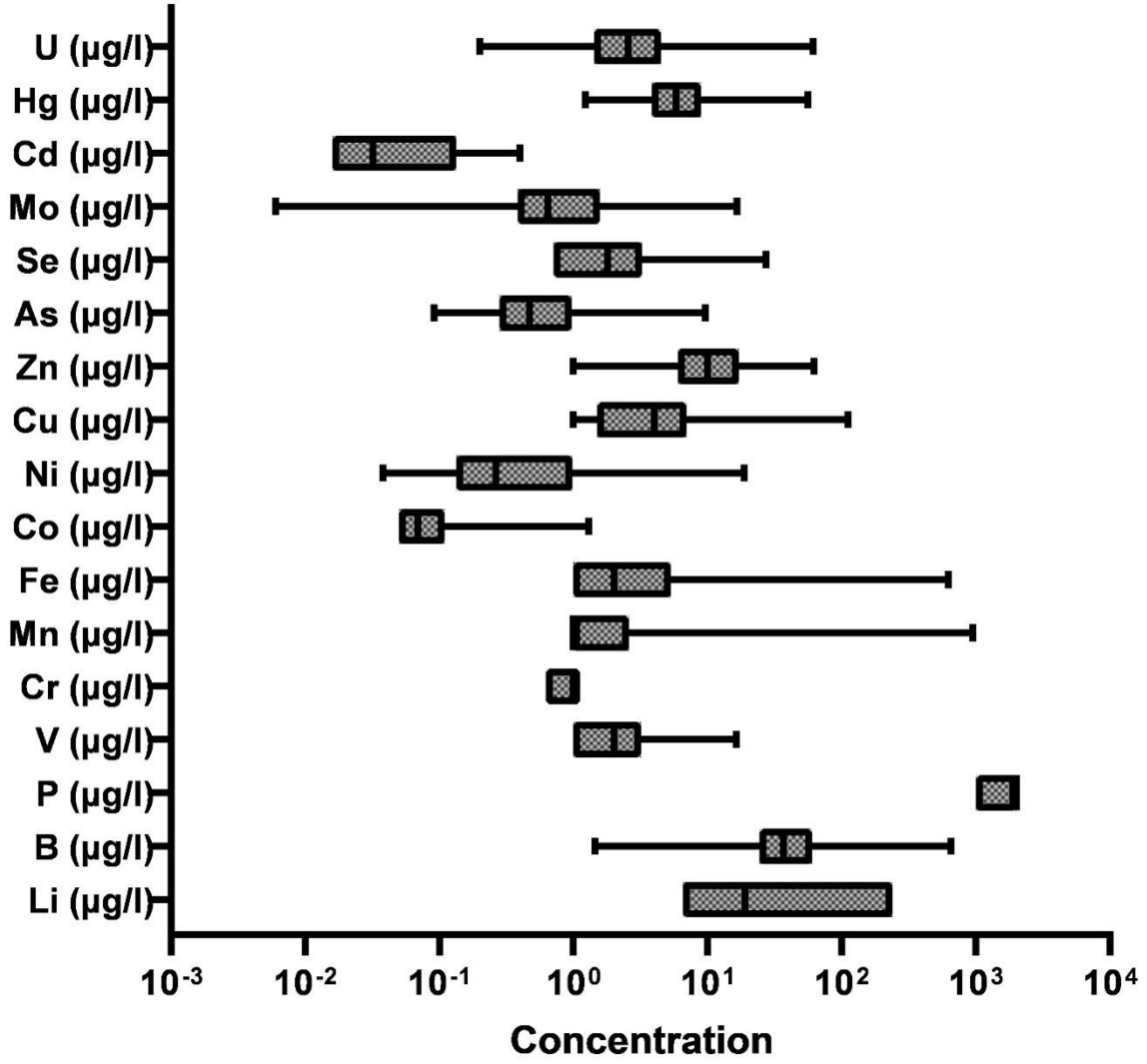

Figure 7. Floating bar graph of trace element concentrations for all wells sampled. The floating bars start at the minimum concentration and go to the maximum, the line at the center of the box is the median concentration value, the box represents interquartile values (between 25th percentile and 75th percentile).

Among the private wells we sampled, five contained chloride concentrations above the secondary MCL, five contained sulfate concentrations above the secondary MCL, and 28 samples out of 63 (45%) had concentrations of nitrate as N above the primary MCL. None of the private well samples contained trace elements in concentrations above primary or secondary MCL's considered in our study.

Using the combined data set of monitoring and private well points, we found that the occurrence of nitrate had a positive correlation with alkalinity, and the concentrations of DO, calcium, strontium, and uranium (Figure 8; Figure 9). Nitrate had a negative correlation with the concentrations of arsenic, and well depth (Figure 8; Figure 9).

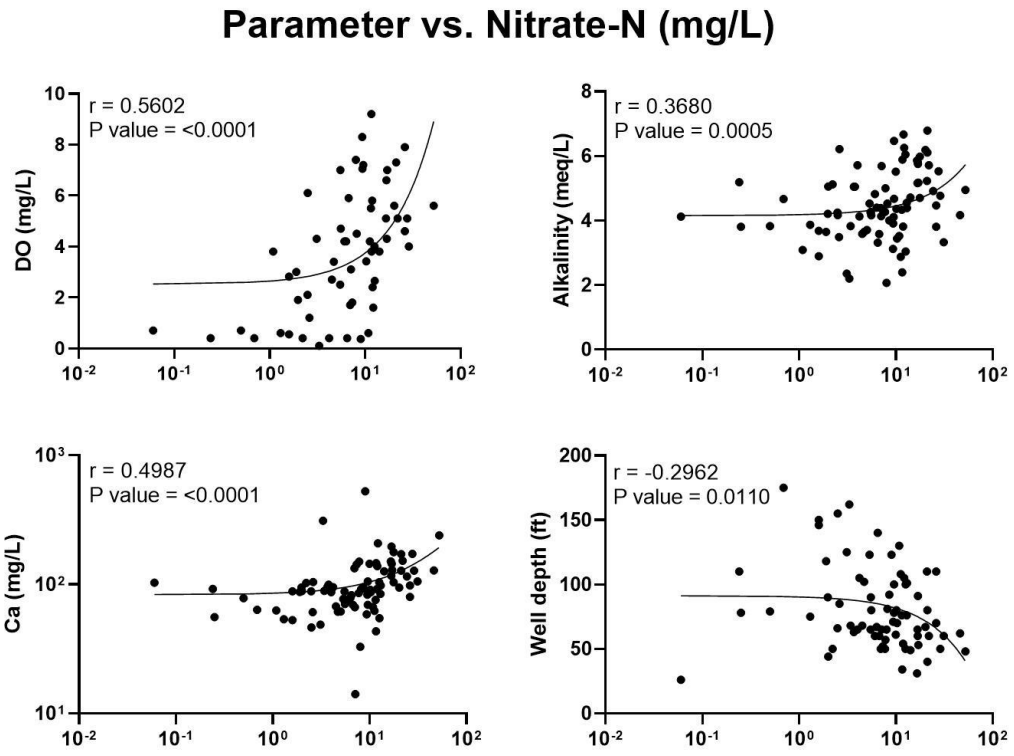

Figure 8. Variation in nitrate concentration with other parameters in our dataset. Only significant correlations are shown. Positive correlations (i.e., as nitrate concentration increases, so does the other parameter) are shown with DO (mg/L), alkalinity (meq/L), calcium (mg/L). Negative correlations (i.e., as nitrate concentration decreases, so does the other parameter) are shown with well depth (ft).

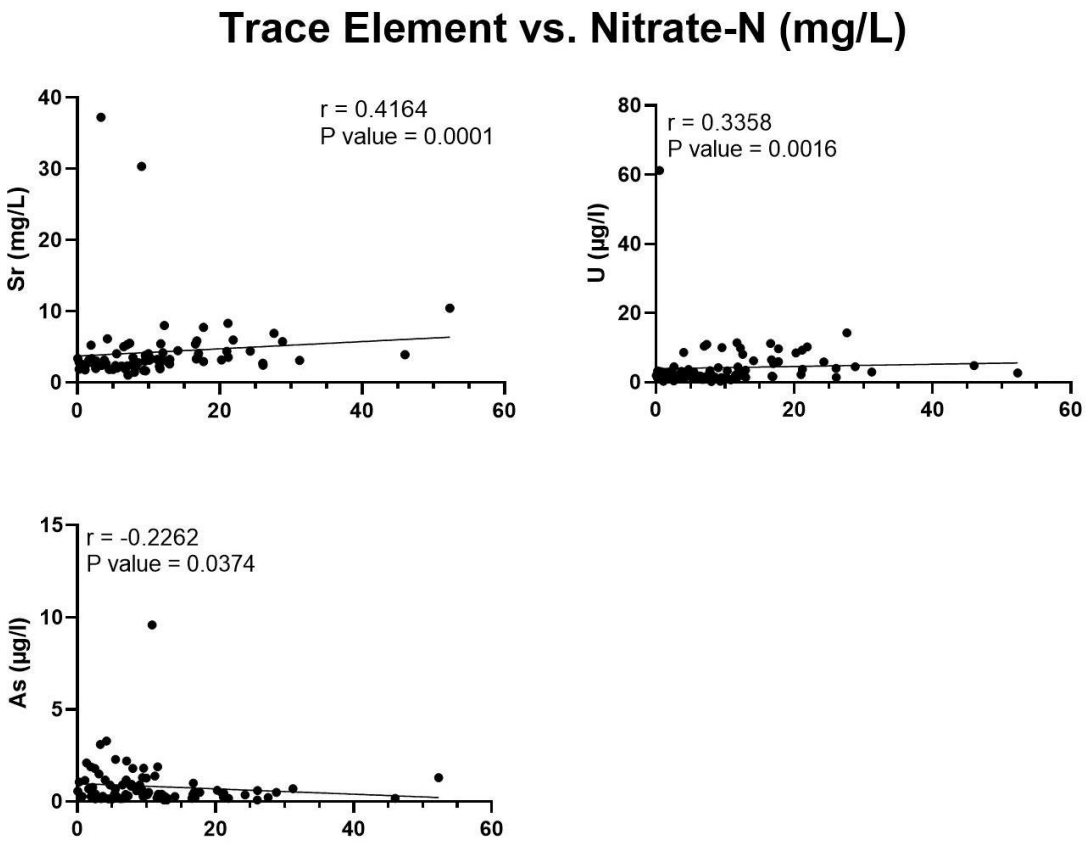

Figure 9. Variation in nitrate concentration with trace elements. Only significant correlations are shown. Positive correlations (i.e., as nitrate concentration increases, so does the other parameter) are shown with strontium (mg/L), and uranium (ug/L). Negative correlations (i.e., as nitrate concentration decreases, so does the other parameter) are shown with arsenic (ug/L).

Land Use/Land Cover

To analyze spatial relationships between water quality parameters and bedrock, and LULC classes, we considered both private and monitoring wells. The percentages of LULC classes in each buffer zone are shown in Table 3, spatial correlation data is shown in Table 4.

Out of the 10 Modified Anderson Level I LULC classifications from the KBS's 2015 Kansas Land Cover Patterns Phase I - Final Report we excluded the Other (60) classification from our results because there were no instances of Other (60) within our dataset.

The type of LULC present changed as buffer size changed. For example, as the buffer zones got smaller, the urban classifications decreased in their percent coverage. The cropland classification generally increased in its percent coverage, except for at the 3000 m buffer zone. Grassland, woodland, and surface water (non-urban) all decreased as the buffer zone size became larger.

In our statistical analysis of the correlations between the percentage of LULC type and the occurrence of nitrate we used the non-parametric Spearman Rank Test. We found a positive correlation between the occurrence of nitrate as N at the 200 m buffer radius and the water (non-urban) classification. We found negative correlations between nitrate as N at the 800 m buffer radius with urban residential, urban openland, and grassland. We found a negative correlation between nitrate and urban openland at the 1000 m buffer radius, and a negative correlation at the 1200 m buffer radius with urban woodland.

Buffer (m)	Urban Indust./Comm. (%)	Urban Residential (%)	Urban Openland (%)	Urban Woodland (%)	Urban Water (%)	Cropland (%)	Grassland (%)	Woodland (%)	Water (%)
100	11.40	66.85	36.92	2.74	0.00	59.27	62.74	12.61	2.47
200	8.03	51.92	26.62	4.31	0.83	67.32	45.25	6.50	1.13
500	6.59	25.19	17.47	2.56	1.56	75.45	26.72	2.51	0.84
800	3.17	9.16	12.62	1.39	0.63	75.27	23.67	1.87	0.67
1000	2.23	7.09	10.47	0.96	0.42	75.63	22.92	1.60	0.56
1200	1.81	5.85	6.12	0.59	0.29	76.12	22.57	1.35	0.44
1500	0.71	2.83	4.40	0.39	0.17	76.45	22.47	1.18	0.45
1800	0.79	2.52	3.81	0.23	0.11	75.80	22.65	1.06	0.42
2500	0.65	1.66	2.54	0.14	0.06	74.70	23.48	1.20	0.43
3000	0.11	0.44	0.59	0.02	0.02	72.53	24.50	1.30	0.48

Table 3. Average percentage of each LU/LC by the radius size for all wells. The dominant LU/LC type is Cropland.

Radius	Urban Indust./Comm.	Urban Residential	Urban Openland	Urban Woodland	Urban Water	Cropland	Grassland	Woodland	Water
200									
800									
1000									
1200									

Table 4. Spearman's Rank negative and positive correlations with all 86 wells, green represents a positive correlation and red represents a negative correlation. 100m, 500m, 1500m, 1800m, 2500m, 3000m had no correlations with nitrate are not shown in this table.

Geospatial Relationships

Out of the private and monitoring wells, 42 are located above Permian bedrock, and 44 lie above Cretaceous bedrock. In our statistical analysis between chloride and bedrock type, we used a Mann-Whitney test to evaluate any statistical correlations or significance. We obtained a P value of 0.0026, indicative of significant correlation between chloride concentrations and Permian bedrock. The average concentration of chloride in wells drilled above Cretaceous bedrock was 81.46 mg/L, the average concentration of chloride wells drilled above Permian bedrock was 642.1 mg/L.

Total well depth data was available for 73 wells, screen interval data was available for 52 wells, and clay lens data was available for 38 out of the 86 private and monitoring wells. The statistical correlations (if any were present) between nitrate as N and well depth and other parameters are shown in Figure 8 and Figure 9.

We also evaluated correlations between the depth of the wells with the water quality parameters using Spearman's Rank Test. We found negative correlations between well depth and alkalinity, and the concentrations of nitrate as N, bromide, magnesium, calcium, uranium. To evaluate the correlation between nitrate as N and well depth, we separated wells into shallow and deep using their median well depth (71ft). Figure 10 shows the correlation in a box plot of nitrate as N concentrations in the deep and shallow wells, shallow wells have a higher average nitrate as N concentration.

The correlation between the thickness of the clay intervals above the well screen and all other parameters were evaluated using the two-tailed Spearman's Rank Test. We found a positive correlation between proportion of clay above the screen and the concentration of potassium, and vanadium. There is a negative correlation between the length of clay and the concentration of uranium.

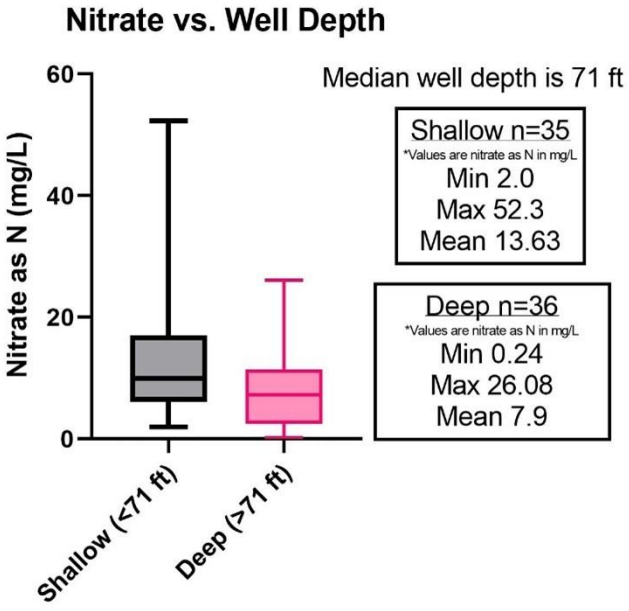

Figure 10. Floating box graph of nitrate as N and well depth. We grouped the wells into deep and shallow classes based on the mean well depth of the wells included in this study.

Chapter 6 - Discussion

Groundwater Mixing and Geologic Controls

Geology is causing some degradation in water quality by adding Permian brine (Whittemore, 1993). By completing a mixing analysis, we can better understand water quality parameters, where they may originate from, and what may be controlling their concentrations. In evaluating correlations between bedrock geology and water quality parameters we may be able find reasoning between correlations among bedrock type, clay lens thickness, and water quality parameters.

Within the GBPA, there are different sources of water that can be identified using bromide and chloride ratios as tracers. Bromide and chloride are good tracers because they are highly soluble conservative ions, which means they do not readily participate in reactions (such as reduction and oxidation reactions) (Whittemore, 1995). Chloride is the best indicator of a water's salinity, which is an important variable in water quality (Whittemore, 1995).

Whittemore (1995) established characteristic concentrations of bromide and chloride in three different water sources within the GBPA. They found that these ratio values in the GBPA are consistent with fresh aquifer water (bromide/chloride ratio of 0.0003 to 0.1), spills/seeps of produced brine from oil and gas well installation and maintenance (bromide/chloride ratio of, 0.0005 to 0.04), and Permian evaporite brine (bromide/chloride ratio of, 0.00006 to 0.0005) (Whittemore, 1995). Using these ratios as a signature, we can begin to identify sources of salinity at the sampling points within the aquifer (Whittemore, 1995). Figure 11 shows the mixing curve established by Whittemore (1993) and our data points, as well as colored regions in which the different source water would plot.

Consistent with Whittemore (1993), and our mixing analysis results, we see chloride concentrations were primarily elevated in the eastern half of the GBPA, where Permian bedrock floors the aquifer (Figure 12). The Permian bedrock is rich in evaporite deposits, halite, and gypsum. Halite and gypsum contain soluble ions like, sodium, chloride, and sulfate, and when dissolved, these ions create a brine. This Permian brine has been known to mix with the GBPA fresh water and cause an increase in salinity (Whittemore, 1993; Buddemeier, 1994; Townsend and Young, 1995).

Out of 75 samples, 63 samples included in our study had bromide/chloride*10,000 ratios within the range of mixing between fresh GBPA water and Permian brine water. Samples BA06 and BA24 lie above the mixing curve for fresh water and Permian brine, they have nitrate as N concentrations of 16.71 (mg/L) and 11.7 (mg/L) respectively. The results at these two locations suggest that there may be combined additions of salinity from evapotranspiration and/or oil and gas brine. More than 450,000 oil and gas wells have been drilled in Kansas since the first was completed in 1892 (KGS, 2022b; Wells and Wells). Therefore, it is likely that over time there has been enough accidental spills of produced brine, leaky brine containers, or negligence in the disposal of produced oil field brine, to cause mixing between oil and gas brines and the GBPA. It is this origin of oil and gas brines that we believe to be another source of salinity in the GBPA.

Water affected by evapotranspiration can also add salinity to the GBPA by the removal of fresh water, and concentration of salts (Whittemore, 1993). We can use the presence of nitrate (grouping concentrations into below and above background values) as a proxy for evapotranspiration, but we know that nitrate is added at the surface (which is where evapotranspiration occurs). A nitrate value above background (4 mg/L) indicates a surficial source of nitrate, and therefore implies that the surficial process of evapotranspiration is also

occurring (Whittemore, 1993). The extent to which evapotranspiration occurs depends on seasonality, as this process begins to affect groundwater composition the most during the warmest months of the year (Jasechko et al., 2014; Phan et al., 2021). Jasechko et al. (2014) determined that in temperate grassland areas (the GBPA area falls under this category) the majority of water recharge from precipitation occurs in the winter months, when evapotranspiration occurs at its lowest capacity. This occurs because surface temperatures are highest during summer months, and plant-life is transpiring and intercepting precipitation (Jasechko et al., 2014).

There are 55 wells in our data set with nitrate as N values above background. Considering these 55 wells that have over 4 mg/L nitrate as N, we can assume that evapotranspiration has also affected the salinity of the water at these points. 35 of these data points have nitrate as N values above the U. S. EPA MCL 10 mg/L. There are 20 wells that have nitrate as N below the background value, this indicates the water at these points has not undergone evapotranspiration. The GBPA as an aquifer is unconfined and exposed at the surface, hence surficial processes can affect salinity.

There are two well points with chloride contamination on the Cretaceous half of the aquifer, KH01 and BA34 (Figure 12). These wells show concentrations of chloride and bromide/chloride*10,000 ratios that plot within the curve of standard mixing between fresh water and Permian brine. However, these wells were not drilled over Permian bedrock. It is possible that these two wells have increased salinity from oil and gas brine spills.

Overall, our results support previous findings in the GBPA, in that there is mixing between fresh aquifer water and Permian brine (Whittemore, 1993, 1995; Lane et al., 2020). Our results also indicate combined mixing of fresh water with oil and gas brine and water affected by

evapotranspiration. It is important to note that all data points used within this study were sampled during May, June, and July during typical warm summers, when evapotranspiration and irrigation rates are highest. These results may then only be representative of groundwater properties during this time of year.

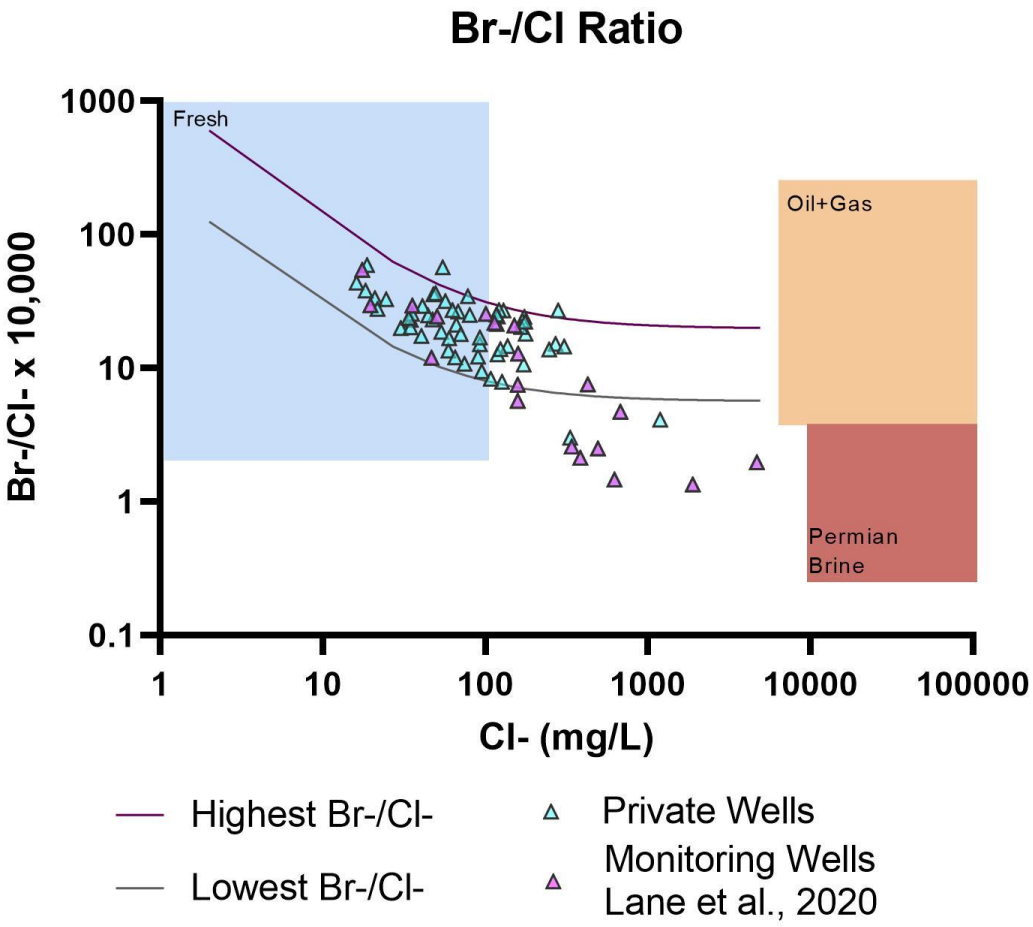

Figure 11. Mixing curve and description of salinity of wells included in our study. Blue data points are freshwater wells, tan triangles are a mix between fresh water and oil and gas brine, and the square data points are a mix of fresh and Permian brine water. Mixing curves calculated using data from Whittemore (1993; 1995).

The presence and variable thicknesses of clay lenses within aquifers can inhibit the downward migration of nitrate as N contaminants (Townsend and Young, 1995). Using available well logs from the interactive Kansas Oil and Gas Map, we found how many feet of clay in each

well existed over the well screen. We did not identify any trends between nitrate as N and clay thickness. There was a positive correlation between thickness of clay lens, potassium, and vanadium. These results might be attributable to higher concentrations of this cation and trace element in the bedrock.

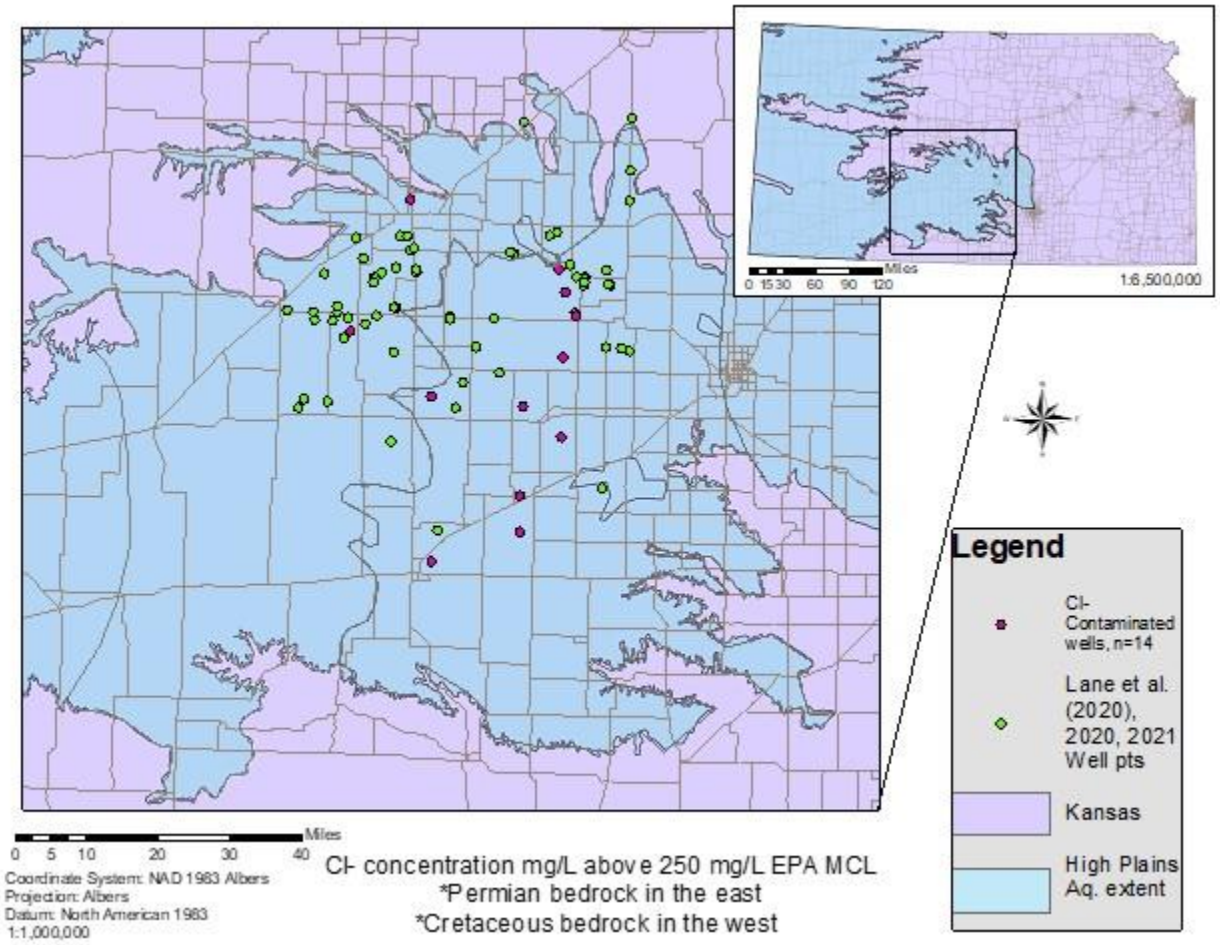

Figure 12. Map of wells considered in this study from 2016 (from Lane et al. 2020), 2020, and 2021. Pink well points have concentrations of chloride above the U. S. EPA's secondary contaminant level. The grey line in the middle of the GBPA is the border between Cretaceous bedrock in the west, and Permian bedrock in the east. Base maps modified from KGS (2012) and ESRI (2021).

Impact of Land Use/Land Cover

Using LULC maps and measured nitrate as N concentrations, we evaluated correlations between LULC and nitrate as N at different buffer radii around each well. In general, cropland represents the highest percentage of land use in the buffer areas we considered. As the buffer radii get larger, there is an increasing percent coverage of cropland, and a decrease in grassland, woodland, surface water (non-urban), and all urban classifications.

There were no correlations between the occurrence of nitrate as N and any LULC at the buffer radii of 100, 500, 1500, 1800, 2500, or 3000 m. The LULC percentages indicated negative correlations between nitrate and urban residential (at the 800 m radius), urban openland (at the 800 m and 1000 m radii), and urban woodland (at the 1200 m radius) and grassland (at the 800 m radius). These negative correlations between urban classifications and nitrate as N suggest that less fertilizers are applied to these LULC types in general, thus the groundwater beneath would also have lower nitrate as N concentrations. In our analysis, there was only one positive correlation between nitrate as N and any land use classification, the correlation was with surface water (non-urban) at the 200m buffer radius. Considering the low average percent stated in the results (1.13% of the land cover was non-urban water) we believe this correlation is coincidental.

Nitrate as N concentrations decreased with well depth. This is because in the GBPA the dominant source of nitrate as N is ammonium-based fertilizers applied at the surface (Lane et al., 2020). As this surficial ammonium enters the subsurface it goes through nitrification and the ammonium oxidizes to produce nitrite (Rivett et al., 2008). Nitrite then becomes oxidized to nitrate (Rivett et al., 2008). The concentration of nitrate thus decreases with depth into the aquifer.

Trace Element Control

Nitrate can act as a control on the release of some toxic trace elements (Gates et al., 2009; Nolan and Weber, 2015). Nolan et al. (2015) found that nitrate affects uranium concentration by aiding in the oxidative dissolution of reduced uranium (IV). Uranium exists naturally in some rock formations, such as black shale (which is present in the GBPA bedrock lithology) (Fader and Stullken, 1978; Nolan and Weber, 2015). The uranium has been locked in the minerals in an immobile state, however, increasing nitrate concentrations (and/or the presence of nitrate in general) may be causing the dissolution and release of uranium into the groundwater (Nolan and Weber, 2015).

To evaluate the control on uranium, we ran Spearman's Rank Tests among nitrate as N concentrations and the trace elements we measured. Our results suggest that nitrate contamination may cause the release of toxic trace elements, as we found a positive correlation between nitrate as N and uranium. The significant positive relationship between nitrate as N and uranium can be attributed to nitrate aiding in the oxidative dissolution of reduced uranium (IV).

Nitrate has also been linked to the propulsion of selenium in groundwater, although we did not observe any trends between nitrate as N and selenium (Gates et al., 2009). We feel it is important to recall that none of the private wells had over the MCL listed by the U. S. EPA for trace elements considered in this study.

The positive relationships between nitrate and alkalinity, calcium, and strontium, are consistent with application of lime on agricultural land. Lime is applied to agricultural land at the surface because it combats soil acidity, which would increase alkalinity in the groundwater (Andreasen and Thomsen, 2021). Strontium is released in the soil by this added lime. (Andreasen and Thomsen, 2021). These positive correlations with nitrate are likely because each of these parameters, nitrate, alkalinity, strontium, and calcium, are mediated by surficial processes, thus

where one parameter is has increasing concentrations, so will the other parameters (Lane et al., 2020; Andreasen and Thomsen, 2021). This is consistent with the negative correlations between these parameters and well depth, as they are surficially added and concentrations decrease with depth into the aquifer.

The negative relationship between nitrate and arsenic may be due to microbial reactions and reduction/oxidation state. Nitrate causes more oxidized environments, and arsenic is more mobile in reducing environments (Zhu et al., 2019). Hence the nitrate may be causing the arsenic to sorb onto minerals and remain in its solid state (Zhu et al., 2019).

Chapter 7 - Conclusions

Our efforts in analyzing the results have confirmed relationships between groundwater quality parameters, and LULC, and bedrock geology and shed light on the origin of salinity in the GBPA. Results of our study suggest there is widespread nitrate contamination in private wells in the GBPA. Since 44% (28 out of the 63) of the private well samples had nitrate contamination, and >33,000 people obtain drinking water from private wells, there is a possibility that >14,666 people (44% of total the total population) have water that would be considered not potable by the US EPA. It is important to recall that this is an estimation, not an exact measurement.

Our results confirm previous findings by Nolan et al. (2015) in that nitrate has positive correlation with the presence of toxic trace elements, uranium. It is important to note that none of the private wells included in this study had uranium concentrations over the U. S. EPA MCL. The analysis of mixing relationships we completed using end members of fresh aquifer water, Permian brine water, and oil-field brine water, indicate that the greatest contributor to salinity in the aquifer is Permian brine.

Our findings demonstrate a need for private well owners to get their water tested and take precautionary steps to better understand and purify their water. The CDC recommends that private wells be tested once a year for total dissolved solids, nitrates, pH, and coliform bacteria (CDC, 2020a). A good option for water purification is under-the-sink reverse osmosis systems. Reverse osmosis is effective at removing harmful concentrations of protozoa, bacteria, viruses, and other dissolved ions including nitrate, and they cost about as much as one complete water quality analysis (approximately $200) (CDC, 2020a, 2020b). Gaining a better understanding of the aquifer's quality in private wells and the aquifer will lead to better educated decisions and

policies created for the goal of prolonged life and healthy human and animal inhabitants of the GBPA.

While many people use domestic wells in the High Plains Aquifer, like the >33,000 in the GBPA, the quality of water within the wells is largely unknown. Our research indicates alarming amounts of nitrate as N and offers insights on relationships among nitrate as N and LULC, trace elements, and bedrock differences. These results highlight the importance of groundwater quality testing and routine monitoring to safeguard the health and safety of private well owners in GBPA.

Chapter 8 - References

Andreasen, R., and Thomsen, E., 2021, Strontium Is Released Rapidly From Agricultural Lime–Implications for Provenance and Migration Studies: Frontiers in Ecology and Evolution, v. 8, p. 588422, doi:10.3389/fevo.2020.588422.

Balleau Groundwater, INC., 2010, Hydrologic Model of Big Bend Groundwater Management District No. 5:, http://archive.gmd5.org/District_Model/GMD5_Model_Final_Report.pdf (accessed August 2021).

Buddemeier, R.W., 1994, Overview and Summary of FY94 Mineral Intrusion Studies: Kansas Geological Survey Open-File 94–28a.

CDC, 2020a, Drinking Water Frequently Asked Questions; Drinking Water; Healthy Water; CDC:, https://www.cdc.gov/healthywater/drinking/drinking-water-faq.html (accessed April 2022).

CDC, 2018, Facts about Cyanobacterial Harmful Algal Blooms for Poison Center Professionals | Harmful Algal Blooms | CDC:, https://www.cdc.gov/habs/materials/factsheet-cyanobacterial-habs.html (accessed February 2022).

CDC, 2020b, Technical Information on Home Water Treatment Technologies; Home Water Treatment; Drinking Water; Healthy Water; CDC:, https://www.cdc.gov/healthywater/drinking/home-water-treatment/household_water_treatment.html (accessed February 2022).

Chapra, SC et al., 2017, Climate Change Impacts on Harmful Algal Blooms in US Freshwaters: A Screening-Level Assessment: Environmental Science & Technology, v. 51, p. 8933–8943, doi:10.1021/acs.est.7b01498.

ESRI, 2021, USA State Boundaries - Overview: arcgis.com, https://www.arcgis.com/home/item.html?id=540003aa59b047d7a1f465f7b1df1950 (accessed April 2022).

Fader, SW, and Stullken, L.E., 1978, Geohydrology of the Great Bend Prairie, South-Central Kansas: Kansas Geological Survey Irrigation Series 4.

Gates, T.K., Cody, B.M., Donnelly, J.P., Herting, A.W., Bailey, R.T., and Mueller Price, J., 2009, Assessing Selenium Contamination in the Irrigated Stream-Aquifer System of the Arkansas River, Colorado: Journal of Environmental Quality, v. 38, p. 2344–2356, doi:10.2134/jeq2008.0499.

Jasechko, S., Birks, S.J., Gleeson, T., Wada, Y., Fawcett, P.J., Sharp, Z.D., McDonnell, J.J., and Welker, J.M., 2014, The pronounced seasonality of global groundwater recharge: Water Resources Research, v. 50, p. 8845–8867, doi:10.1002/2014WR015809.

Kansas Water Authority, 2022, Annual Report to the Governor and Legislature: Kansas Water Authority Annual Report 2022.

KGS, 2012, High Plains Aquifer Regions in Kansas: Kansas Geological Survey, Kansas University, https://geokansas.ku.edu/kansas-high-plains-aquifer-atlas.

KGS, 2022a, Kansas Oil and Gas; Kansas Water Well Interactive Map: Kansas Geological Survey, Kansas University, https://maps.kgs.ku.edu/oilgas/index.html.

KGS, 2022b, Oil and gas production in Kansas; GeoKansas:, https://geokansas.ku.edu/oil-and-gas-production-kansas (accessed April 2022).

KGS, 1998, Regional Stratigraphy of the Dakota Formation, Kiowa Formation, and Cheyenne Sandstone in Kansas:, https://www.kgs.ku.edu/Dakota/vol3/fy89/index.htm (accessed March 2022).

KS-EPHT, and KDHE, 2017, Kansas 2017 Harmful Algal Bloom Summary: Kansas Environmental Public Health Tracking Program.

Lane, A.D., Kirk, M.F., Whittemore, D.O., Stotler, R., Hildebrand, J., and Feril, O., 2020, Long-term (1970s–2016) changes in groundwater geochemistry in the High Plains aquifer in south-central Kansas, USA: Hydrogeology Journal, v. 28, p. 491–501, doi:10.1007/s10040-019-02083-z.

Mudge, M. R., McKee, E. D., and Oriel, S. S., 1967, Chapter F, central midcontinent region; in, Paleotectonic Investigations of the Permian System in the United States: US Geological Survey, Professional Paper 515-F, p. 93-123.

Nolan, J., and Weber, K.A., 2015, Natural Uranium Contamination in Major U.S. Aquifers Linked to Nitrate: Environmental Science & Technology Letters, v. 2, p. 215–220, doi:10.1021/acs.estlett.5b00174.

Peterson, D.L., and Egbert, S.E., 2017, 2015 Kansas Land Cover Patterns Phase I: Final Report: University of Kansas Final 23.

Phan, V.A., Zeigler, K.E., and Vinson, D.S., 2021, High Plains groundwater isotopic composition in northeastern New Mexico (USA): relationship to recharge and hydrogeologic setting: Hydrogeology Journal, v. 29, p. 1445–1461, doi:10.1007/s10040-021-02329-9.

Rivett, M.O., Buss, S.R., Morgan, P., Smith, J.W.N., and Bemment, C.D., 2008, Nitrate attenuation in groundwater: a review of biogeochemical controlling processes: Water Research, v. 42, p. 4215–4232, doi:10.1016/j.watres.2008.07.020.

Townsend, M.A., and Young, D.P., 1995, Factors Affecting Nitrate Concentrations in Ground Water in Stafford County, Kansas: Current Research in Earth Sciences, p. 1–9, doi:10.17161/cres.v0i238.11844.

US EPA, 2015, Chemical Contaminant Rules: https://www.epa.gov/dwreginfo/chemical-contaminant-rules (accessed February 2022).

US EPA, O., 2013, The Effects: Dead Zones and Harmful Algal Blooms: https://www.epa.gov/nutrientpollution/effects-dead-zones-and-harmful-algal-blooms (accessed February 2022).

USGS, 2012, Web-based Alkalinity Calculator: Oregon Water Science Center; Alkalinity Calculator, https://or.water.usgs.gov/alk/ (accessed February 2022).

Wells, B.A., and Wells, K.L. Article Title: "First Kansas Oil Well." Authors: B.A. Wells and K.L. Wells. Website Name: American Oil & Gas Historical Society. https://aoghs.org/petroleum-pioneers/kansas-mid-continent-oil-fields. Last Updated: June 24, 2021. Original Published Date: June 19, 2014.:

West, R.R., Miller, K.B., and Watney, WL, 2010, The Permian System in Kansas: Kansas Geological Survey Bulletin 257, 88 p.

Whittemore, D., 1995, Geochemical differentiation of oil and gas brine from other saltwalter sources contaminating water resources: Case studies from Kansas and Oklahoma: Environmental Geosciences, v. 2, p. 15–31.

Whittemore, D.O., 1993, Ground-Water Geochemistry in the Mineral Intrusion Area of Groundwater Management District No. 5, South-Central Kansas: Kansas Geological Survey Open-File.

Whittemore, D.O., Butler, J.J., and Wilson, B.B., 2018, Status of the High Plains Aquifer in Kansas: Kansas Geological Survey Technical Series 22.

Whittemore, D.O., Macfarlane, PA, and Wilson, B.B., 2014, Water Resources of the Dakota Aquifer in Kansas: Kansas Geological Survey Bulletin 260, 68 p.

Whittemore, D.O., Sophocleous, M.A., and Buddemeier, R.W., 1992, Mineral Intrusion: Investigation of Salt Contamination of Ground Water in the Eastern Great Bend Prairie Aquifer: Kansas Geological Survey, Open-file Report 92-25, http://www.kgs.ku.edu/Hydro/Publications/1992/OFR92_25/index.html (accessed August 2021).

Zamyadi, A., MacLeod, S.L., Fan, Y., McQuaid, N., Dorner, S., Sauvé, S., and Prévost, M., 2012, Toxic cyanobacterial breakthrough and accumulation in a drinking water plant: A monitoring and treatment challenge: Water Research, v. 46, p. 1511–1523, doi:10.1016/j.watres.2011.11.012.

Zhu, X., Zeng, X.-C., Chen, X., Wu, W., and Wang, Y., 2019, Inhibitory effect of nitrate/nitrite on the microbial reductive dissolution of arsenic and iron from soils into pore water: Ecotoxicology, v. 28, p. 528–538, doi:10.1007/s10646-019-02050-0.

Appendix A - Geochemistry

Sample ID	Affiliation	Date	Latitude	Long	Permian/Cretaceous	pH	T (c)
BA01	Private	6/11/21	38.16137	-99.01186	C	7.47	18.9
BA02	Private	6/11/21	38.16185	-98.95095	C	7.32	15.7
BA03	Private	6/11/21	38.11088	-98.93091	C	7.08	16.2
BA04	Private	6/11/21	38.1455	-99.00787	C	7.03	16.7
BA05	Private	6/11/21	38.14522	-98.96074	C	7.09	15.4
BA06	Private	6/12/21	37.96957	-99.04239	C	7.34	15.9
BA07	Private	6/12/21	37.98631	-99.02798	C	7.38	16.9
BA08	Private	6/12/21	37.98367	-98.96729	C	7.48	17.1
BA09	Private	6/12/21	38.15236	-98.92146	C	7.32	15.6
BA10	Private	6/12/21	38.23483	-98.85713	C	7.16	15.5
BA11	Private	6/12/21	38.238	-98.84861	C	7.1	15.5
BA12	Private	6/12/21	38.22388	-98.8585	C	7.08	17.2
BA13	Private	6/12/21	38.24353	-98.83845	C	7.02	15.7
BA14	Private	6/12/21	38.27057	-98.88669	C	7.22	15.7
BA15	Private	6/13/21	38.28923	-98.76544	C	7.3	15.8
BA16	Private	6/13/21	38.3183	-98.79261	C	7.46	16.2
BA17	Private	6/13/21	38.31859	-98.79236	C	7.53	15.5
BA18	Private	6/13/21	38.31753	-98.77408	C	7.44	16.1
BA19	Private	6/13/21	38.31905	-98.77489	C	7.16	15.3
KH01	Private	6/11/21	38.12475234	-98.91387193	C	7.08	25.8
KH02	Private	6/11/21	38.14020454	-98.87633248	C	7.16	20.8
KH03	Private	6/11/21	38.17449277	-98.79761815	C	7.33	20.4
KH04	Private	6/11/21	38.29504504	-98.75630039	C	7.11	17.2
KH05	Private	6/11/21	38.24781322	-98.74785675	C	7.34	17.2
KH06	Private	6/12/21	38.25201742	-98.74873246	C	7.5	17.7
KH07	Private	6/12/21	38.15913051	-98.65737269	P	7.24	17
KH08	Private	6/12/21	38.0295	-98.619556	P	7.14	18.4
KH09	Private	6/12/21	37.97839787	-98.63712302	P	7.3	18
KH10	Private	6/12/21	38.0509623	-98.52720433	P	7.75	18
KH11	Private	6/13/21	38.10048511	-98.58970566	P	7.35	18.4
KH12	Private	6/13/21	38.29098179	-98.50633822	C	7.3	15.7
KH13	Private	6/13/21	38.29189058	-98.50634025	C	7.28	16.9
KH14	Private	6/13/21	38.28927929	-98.49754074	C	7.29	17
KH15	Private	7/18/20	38.460556	-98.200556	P	7	21.6
KH16	Private	7/18/20	38.155278	-98.657222	P	7.35	19.7
KH17	Private	7/18/20	38.552778	-98.481111	C	7.32	19.9
KH18	Private	7/18/20	38.168333	-98.333333	P	7.48	20.4
KH19	Private	7/18/20	38.333333	-98.3875	C	7.31	22.8
KH20	Private	7/18/20	38.3275	-98.406389	C	7.36	26.3
KH21	Private	7/18/20	38.311667	-98.906111	C	7.05	21.2
KH22	Private	7/18/20	38.291111	-98.506389	C	7.68	22.8
KH23	Private	7/18/20	38.163056	-99.079167	C	7.33	25.6
KH24	Private	7/18/20	38.157778	-98.848333	C	7.36	20.2
KH25	Private	7/18/20	38.565278	-98.200556	P	7.22	27.1
KH26	Private	7/18/20	38.399722	-98.201111	P	7.23	n.d.
KH27	Private	7/18/20	38.238333	-98.985833	C	7.33	25.8
BA20	Private	6/25/21	38.24526	-98.31249	P	7.53	15.8
BA21	Private	6/25/21	38.24423	-98.31312	P	7.5	16
BA22	Private	6/26/21	38.2296363	-98.3156875	P	7.31	14.3
BA23	Private	6/26/21	38.2456831	-98.33385238	P	7.32	15.6

Sample ID	Affiliation	Date	Latitude	Long	Permian/Cretaceous	pH	T (c)
BA24	Private	6/26/21	38.2594582	-98.3803313	P	7.25	15.5
BA25	Private	6/26/21	38.26906	-98.35057	P	7.16	15.4
BA26	Private	6/26/21	38.26043	-98.25703	P	7.16	21.1
BA27	Private	6/26/21	38.1736871	-98.3357	P	7	16.4
BA28	Private	6/26/21	38.23045	-98.24555	P	7.37	16.7
BA29	Private	6/26/21	38.15822	-98.54438	P	7.59	15.3
BA30	Private	6/26/21	38.10619	-98.25322	P	7.11	15.3
BA31	Private	6/26/21	38.09977	-98.19324	P	7.16	16
BA32	Private	6/26/21	38.10582	-98.21457	P	7.31	16.6
BA33	Private	6/27/21	38.23591	-98.3125	P	7.32	14.9
BA34	Private	6/27/21	38.39118	-98.76897	C	7.12	16
BA35	Private	6/27/21	38.21485	-98.3616	P	7.1	15.2
BA36	Private	6/27/21	38.23205	-98.25006	P	7.36	15.3
10C	KGS	6/22/16	37.98463833	-98.46341833	P	7.33	17.7
21B	KGS	5/31/16	37.8065407	-98.4661394	P	7.24	16.3
26B	KGS	6/2/16	38.0852	-98.36388	P	7.2	16.1
29B	KGS	6/2/16	37.92546	-98.3635	P	7.76	17.4
35B	KGS	6/1/16	37.7335133	-98.4637948	P	7.51	17.4
42B	KGS	6/23/16	37.669869	-98.68812783	P	7.31	17.1
50B	KGS	6/24/16	38.25486	-98.80175	C	7.34	18.2
6B	KGS	6/3/16	37.90806	-98.80147	C	7.43	16.9
BB5HA	KGS	6/23/16	37.99980167	-98.70102167	P	7.5	17.7
10D	KGS	6/22/16	37.98471333	-98.463415	P	7.43	17.5
21C	KGS	5/31/16	37.8065407	-98.4661394	P	6.81	15.2
26C	KGS	6/1/16	38.0852	-98.36388	P	7.57	15.8
29C	KGS	6/2/16	37.92546	-98.3635	P	7.02	17.1
34B	KGS	6/1/16	37.8257	-98.25515	P	7.58	16.6
35C	KGS	5/31/16	37.7335133	-98.4637948	P	7.16	16.1
36D	KGS	6/1/16	37.73284	-98.67576833	P	7.33	16.1
42C	KGS	6/23/16	37.66988967	-98.68812283	P	7.43	16.6
50C	KGS	6/24/16	38.25486	-98.80175	C	7.02	15.9
51B	KGS	6/22/16	38.17511	-98.80395	C	7.29	15.9
52B	KGS	6/22/16	38.08597	-98.80146	C	7.34	17.4
6C	KGS	6/3/16	37.90806	-98.80147	C	7.45	16.3
BB5HB DUP	KGS	6/23/16	37.99980667	-98.70107	P	7.51	16.5
BB8	KGS	6/23/16	38.17369	-98.95028	C	7.54	15.8
BA FieldBlank							

	Conductivity	DO	DO	Specific Conductance	Alkalinity	
Sample ID	(µS/cm)	(mg/L)	(%sat)	(µS/cm)	(meq/L)	(mg/L as CaCO3)
BA01	598.3	4.6	56	713	3.81	190.9
BA02	853.1	0.4	4	977	4.67	233.5
BA03	704.9	7.9	87	805	4.47	223.8
BA04	1071	7.3	81	1160	6.79	339.9
BA05	814.1	4	43	855	6.05	302.9
BA06	740.2	6.6	73	904	5.16	258.2
BA07	554.5	5.5	61	599	4.34	217.2
BA08	617.6	2.7	30	630	3.59	179.4
BA09	877	1.9	20	915	4.21	210.7
BA10	587.5	4.2	45	619	4.4	220
BA11	559.6	4.7	51	588	4.16	208.2
BA12	638.6	2.1	24	693	4.25	212.6
BA13	599.4	4.2	46	663	4.82	241.2
BA14	891.5	5.6	61	931	6.19	309.8
BA15	681.3	2.5	27	719	4.26	213.3
BA16	839.7	1.2	13	903	6.22	311.5
BA17	728.1	0.4	5	794	5.19	259.9
BA18	955.7	0.4	4	1006	5.12	256.3
BA19	1311	2.4	26	1423	6.67	334
KH01	n.d.	n.d.	n.d.	n.d.	5	250.4
KH02	772.1	n.d.	n.d.	n.d.	3.81	190.5
KH03	494.5	n.d.	n.d.	n.d.	4.7	235
KH04	737	n.d.	n.d.	n.d.	5.05	252.7
KH05	n.d.	n.d.	n.d.	n.d.	3.83	191.8
KH06	891.9	n.d.	n.d.	n.d.	4.17	208.8
KH07	734.9	n.d.	n.d.	n.d.	4.68	234.1
KH08	1307	n.d.	n.d.	n.d.	4.39	219.8
KH09	746.2	n.d.	n.d.	n.d.	4.36	218.3
KH10	753.9	n.d.	n.d.	n.d.	5.72	286.1
KH11	658.4	n.d.	n.d.	n.d.	4.27	213.7
KH12	871.5	n.d.	n.d.	n.d.	5.05	252.8
KH13	890.1	n.d.	n.d.	n.d.	3.71	185.8
KH14	769.3	n.d.	n.d.	n.d.	3.33	166.7
KH15	n.d.	n.d.	n.d.	n.d.	5.81	290.9
KH16	n.d.	n.d.	n.d.	n.d.	4	200.2
KH17	n.d.	n.d.	n.d.	n.d.	5.23	261.9
KH18	n.d.	n.d.	n.d.	n.d.	5.06	253.1
KH19	n.d.	n.d.	n.d.	n.d.	4.53	226.8
KH20	n.d.	n.d.	n.d.	n.d.	4.14	207.4
KH21	n.d.	n.d.	n.d.	n.d.	5.98	299
KH22	n.d.	n.d.	n.d.	n.d.	4.11	205.6
KH23	n.d.	n.d.	n.d.	n.d.	4.92	246
KH24	n.d.	n.d.	n.d.	n.d.	4.55	227.5
KH25	n.d.	n.d.	n.d.	n.d.	3.49	174.8
KH26	n.d.	n.d.	n.d.	n.d.	5.52	276.4
KH27	n.d.	n.d.	n.d.	n.d.	6.11	306
BA20	1449	1.8	20	1642	4.33	216.7
BA21	1480	1.7	19	1678	4.39	219.4
BA22	1518	5.1	55	1517	5.53	276.6
BA23	1374	5.1	55	1517	5.86	293.2

	Conductivity	DO	DO	Specific Conductance	Alkalinity	
Sample ID	(µS/cm)	(mg/L)	(%sat)	(µS/cm)	(meq/L)	(mg/L as CaCO3)
BA24	1684	3.8	41	1896	5.89	294.8
BA25	1112	7.2	77	1221	6.47	323.9
BA26	821.5	5.8	69	873	3.82	191.2
BA27	469.1	8.3	91	491	3.12	156.2
BA28	1048	7	77	1118	5.18	259.1
BA29	567.2	3.8	41	573	3.09	154.8
BA30	602.7	4.5	48	604	4.53	226.7
BA31	905.2	4.3	46	920	5.76	288.3
BA32	426.3	5.9	65	428.2	3.58	178.9
BA33	1286	5.1	54	1370	5.72	286.1
BA34	1977	1.6	17	2176	6.26	313.3
BA35	1532	0.7	8	1637	4.12	206.2
BA36	1190	3.8	41	1202	4.72	236.1
10C	2780	0.4	n.d.	n.d.	4.13	206.5
21B	6540	3	n.d.	n.d.	3.65	182.5
26B	36900	0.37	n.d.	n.d.	3.99	199.9
29B	1650	4.3	n.d.	n.d.	2.36	118.2
35B	2600	6.1	n.d.	n.d.	4.17	208.6
42B	15040	0.1	n.d.	n.d.	2.2	110.1
50B	639	0.6	n.d.	n.d.	3.52	176.3
6B	873	2.82	n.d.	n.d.	2.9	145.3
BB5HA	2170	0.4	n.d.	n.d.	3.32	166.4
10D	886	0.7	n.d.	n.d.	3.83	191.5
21C	2170	5.6	n.d.	n.d.	4.95	248
26C	2180	3.1	n.d.	n.d.	5.69	284.6
29C	331	7.4	n.d.	n.d.	2.07	103.6
34B	373	9.2	n.d.	n.d.	2.4	120.3
35C	759	7.05	n.d.	n.d.	3.91	195.9
36D	811	7	n.d.	n.d.	4.27	213.8
42C	901	4.2	n.d.	n.d.	2.88	144.2
50C	1095	4	n.d.	n.d.	4.77	238.9
51B	484	2.65	n.d.	n.d.	3.04	152.2
52B	483	3.4	n.d.	n.d.	3.65	182.7
6C	1032	3.42	n.d.	n.d.	3.44	172
BB5HB DUP	575	0.6	n.d.	n.d.	3.87	193.5
BB8	557	0.55	n.d.	n.d.	3.68	184.4
BA FieldBlank						

Sample ID	Fluoride (mg/L)	Chloride (mg/L)	Nitrite (mg/L)	Bromide (mg/L)	Nitrate (mg/L)	Nitrate as N (mg/L as N)	Sulfate (mg/L)	Sodium (mg/L)
BA01	0.32	30.22	n.a.	0.06	115.42	26.08	23.65	32.92
BA02	0.73	126.76	BDL	0.1	3.05	0.69	81.31	115.3
BA03	0.37	34.84	n.a.	0.08	115.23	26.04	27.44	47.13
BA04	0.28	78.07	n.a.	0.27	93.69	21.17	92.78	97.84
BA05	0.44	47.78	n.a.	0.17	55.51	12.54	46.78	60.13
BA06	0.35	54.53	n.a.	0.31	73.97	16.71	41.25	39.96
BA07	0.45	18.68	n.a.	0.11	50.93	11.51	21.61	33.26
BA08	0.51	49.42	n.a.	0.18	19.84	4.48	24.79	50.51
BA09	0.41	129.53	n.a.	0.35	8.77	1.98	30.27	66.27
BA10	0.38	20.89	n.a.	0.07	28.07	6.34	40.7	34.36
BA11	0.36	16.09	n.a.	0.07	24.69	5.58	29.68	32.31
BA12	0.3	59.09	n.a.	0.08	11.02	2.49	29.41	31.77
BA13	0.32	35.36	n.a.	0.09	26.87	6.07	37.8	42.04
BA14	0.55	24.49	n.a.	0.08	89.64	20.25	50.19	71.09
BA15	0.39	56.67	n.a.	0.18	24.28	5.49	30.17	54.71
BA16	0.51	68.12	n.a.	0.18	11.57	2.61	74.27	54.49
BA17	0.51	62.71	n.a.	0.17	1.06	0.24	62.25	48.29
BA18	0.44	121.31	n.a.	0.33	9.85	2.22	57.27	77.73
BA19	0.33	174.24	n.a.	0.42	53.15	12.01	67.5	118.28
KH01	0.34	270.25	n.a.	0.41	34.61	7.82	43.04	126.91
KH02	0.44	109.37	n.a.	BDL	1.09	0.25	18.84	107.5
KH03	0.42	53.62	n.a.	0.1	78.37	17.71	27.71	42.22
KH04	0.39	137.15	n.a.	0.2	16.3	3.68	36.63	80.17
KH05	0.32	117.15	n.a.	0.25	15.11	3.41	13.32	53.23
KH06	0.36	59.85	n.a.	0.1	203.7	46.02	34.81	43.26
KH07	0.22	34.68	n.a.	0.07	42.41	9.58	17.44	74.79
KH08	0.38	74.29	n.a.	0.08	57.48	12.99	33.94	72
KH09	0.41	94.97	n.a.	0.09	44.79	10.12	39.76	91.16
KH10	0.39	66.26	n.a.	0.14	17.79	4.02	25.02	60.86
KH11	0.34	80.32	n.a.	0.2	34.24	7.74	33.88	63.55
KH12	0.47	90.03	n.a.	0.11	16.74	3.78	41.71	68.17
KH13	0.4	21.72	n.a.	0.06	22.26	5.03	17.37	24.96
KH14	0.31	40.29	n.a.	0.07	123.24	31.21	19.23	24.44
KH15	0.22	246.41	n.a.	0.34	74.27	16.78	52.22	57.57
KH16	0.3	47.46	n.a.	0.11	37.78	8.54	21.03	19.89
KH17	0.41	92.56	n.a.	0.14	92.87	20.98	19.34	29.71
KH18	0.38	1191.35	n.a.	0.49	8.87	2	132.99	717.64
KH19	0.29	30.84	n.a.	BDL	23.62	5.34	13.24	36.49
KH20	0.28	9.87	n.a.	BDL	31.15	7.04	16.84	19.04
KH21	0.49	176.78	n.a.	0.32	78.34	17.7	274.72	127.34
KH22	0.43	107.96	n.a.	0.09	41.91	9.47	32.15	77.2
KH23	1.26	44.43	n.a.	0.11	107.5	24.29	95.6	40.41
KH24	0.41	33.81	n.a.	0.08	57.33	12.95	27.29	40.14
KH25	0.25	41.09	n.a.	0.12	11.44	2.58	45.21	38.28
KH26	0.22	118.74	n.a.	0.15	44.16	9.98	32.37	29.08
KH27	0.72	119.37	n.a.	0.29	93.57	21.14	411.46	134.14
BA20	0.42	168.47	n.a.	0.38	32.52	7.35	278.66	153.17
BA21	0.54	165.86	n.a.	0.34	30.92	6.98	301.04	161.63
BA22	1.2	171.75	n.a.	0.18	122.21	27.61	215.53	112.8
BA23	0.62	176.1	n.a.	0.39	73.32	16.57	144.11	117.61

Sample ID	Fluoride (mg/L)	Chloride (mg/L)	Nitrite (mg/L)	Bromide (mg/L)	Nitrate (mg/L)	Nitrate as N (mg/L as N)	Sulfate (mg/L)	Sodium (mg/L)
BA24	0.49	280.15	n.a.	0.76	51.77	11.7	122.91	174.11
BA25	0.64	117.11	n.a.	0.29	42.29	9.56	47.86	97.02
BA26	0.3	65.23	n.a.	0.08	52.47	11.85	91	55.89
BA27	0.23	24.97	n.a.	BDL	41.25	9.32	13.24	27.58
BA28	0.43	70.44	n.a.	0.13	75.37	17.03	126.78	66.79
BA29	0.05	66.87	n.a.	BDL	4.81	1.09	10.49	44.04
BA30	0.08	18.33	n.a.	0.07	36.14	8.16	17.29	24.27
BA31	0.13	73.32	n.a.	BDL	74.88	16.92	20.15	36.09
BA32	0.27	3.02	n.a.	BDL	29.68	6.71	5.22	9.06
BA33	0.62	123.93	n.a.	0.17	96.86	21.88	156.93	75.29
BA34	0.3	306.17	n.a.	0.44	54.01	12.2	307.77	192.8
BA35	0.22	333.2	n.a.	0.10	BDL	0.06	53.93	207.81
BA36	0.57	92.37	n.a.	0.16	62.39	14.1	164.94	86.07
10C	0.5	676.9	BDL	0.32	18.5	4.2	88.9	419.8
21B	0.5	1885.5	n.a.	0.25	8.2	1.9	202.6	1135.7
26B		12958.4	n.a.	BDL	39.8	9	1274.9	7816.9
29B	0.4	384.3	n.a.	0.08	13.5	3.1	47.1	244.9
35B	0.3	621.9	n.a.	0.09	11	2.5	50.5	417.6
42B	0.9	4682.4	n.a.	0.92	14.7	3.3	1028.2	2840.1
50B	0.5	50.6	n.a.	0.12	48	10.8	36.4	57
6B	0.3	158.2	n.a.	0.12	7.3	1.6	19.6	45.2
BB5HA	0.4	492.8	n.a.	0.12	28.6	6.5	51.7	302.2
10D	0.4	151.1	n.a.	0.32	2.1	0.5	34.4	78.3
21C	0.2	340.1	n.a.	0.09	231.5	52.3	22.3	43.6
26C	0.6	427.4	n.a.	0.32	31.3	7.1	52.9	410.7
29C	0.3	8.6	n.a.	BDL	35.5	8	14.1	18.4
34B	0.4	5.1	n.a.	BDL	51.3	11.6	15.2	11.7
35C	0.2	82	n.a.	BDL	41.6	9.4	13.6	23.2
36D	0.3	100.7	n.a.	0.26	24.5	5.5	16	40.8
42C	0.3	158.4	n.a.	0.09	49.6	11.2	30.7	90.8
50C	0.3	113.5	n.a.	0.25	127.7	28.8	55.9	48.5
51B	0.5	17.5	n.a.	0.09	55.6	12.6	19.8	36
52B	0.4	19.6	n.a.	0.06	20.8	4.7	13.7	23.7
6C	0.3	159.4	n.a.	0.2	45.8	10.3	29.3	78.2
BB5HB DUP	0.4	46.7	n.a.	0.06	6	1.3	17.9	49
BB8	0.5	35.5	n.a.	0.1	6.9	1.6	28.9	40
BA FieldBlank	n.a.	3.38	n.a.	n.a.	0.31	0.07	0.6	n.a.

Sample ID	Ammonium (mg/L)	Potassium (mg/L)	Magnesium (mg/L)	Calcium (mg/L)	Strontium (mg/L)	Li (µg/l)	B (µg/l)	P (µg/l)
BA01	n.a.	3.38	11.06	79.96	2.41	8.758	25.219	BDL
BA02	0.5	3.83	15.57	63.48	2.48	18.71	47.491	BDL
BA03	n.a.	4.04	9.13	98.08	2.68	12.119	29.433	BDL
BA04	n.a.	4.38	13.51	127.42	3.5	12.159	76.115	BDL
BA05	n.a.	4.24	11.79	103.82	2.99	16.43	30.111	BDL
BA06	n.a.	4.34	10.7	116.16	3.28	11.9	24.493	BDL
BA07	n.a.	6.76	6.26	75.68	2.24	9.897	28.785	BDL
BA08	n.a.	3.97	5.15	67.45	1.8	11.001	25.4	BDL
BA09	n.a.	4.79	8.13	94.55	2.82	12.207	27.063	BDL
BA10	n.a.	3.3	8.53	78.5	2.26	10.54	23.759	BDL
BA11	n.a.	3.19	7.97	70.42	2.03	9.286	23.3	BDL
BA12	n.a.	3.58	8.74	88.13	2.49	10.56	20.937	BDL
BA13	n.a.	4	8.41	74.93	2.26	10.08	20.867	BDL
BA14	n.a.	29.94	17.22	94.09	3.16	12.874	51.333	BDL
BA15	n.a.	3.61	7.99	77.25	2.19	8.717	29.785	BDL
BA16	n.a.	3.8	13.31	104.1	3.03	13.452	30.407	BDL
BA17	n.a.	3.35	12.05	91.97	2.82	12.096	25.03	BDL
BA18	BDL	4.27	12.49	102.44	3.06	13.47	26.422	BDL
BA19	0.5	4.45	17.31	138.13	4.14	16.989	46.352	BDL
KH01	0.84	5.75	11.29	149.64	3.48	15.904	34.915	BDL
KH02	1.05	6.25	6.91	55.72	1.85	BDL	1.448	BDL
KH03	n.a.	15.33	9.05	103.6	2.9	10.76	29.067	BDL
KH04	0.38	16.4	8.22	95.66	2.7	10.75	29.337	BDL
KH05	BDL	16.14	7.44	89.08	2.39	7.344	17.722	BDL
KH06	0.26	14.17	12.53	116.16	3.87	11.863	36.452	BDL
KH07	0.38	8.37	4.7	69.36	1.61	6.6	19.33	BDL
KH08	0.48	4.14	9.62	97.74	3.21	12.552	38.337	BDL
KH09	0.47	4.55	10.01	90.83	3.11	11.8	38.222	BDL
KH10	BDL	25.11	7.24	86.81	2.64	12.719	38.244	BDL
KH11	0.29	8.19	8.92	85.71	2.51	9.519	32.659	BDL
KH12	0.45	11.1	12.78	99.56	3.11	12.215	39.426	BDL
KH13	n.a.	10.05	4.75	61.59	1.81	9.117	23.8	BDL
KH14	BDL	17.82	8.38	105.51	3.09	8.035	22.133	BDL
KH15	n.a.	2.9	15.37	195.98	5.8	16.193	22.785	BDL
KH16	n.a.	4.34	5.49	94.95	2.76	9.309	22.756	BDL
KH17	n.a.	2.63	14.09	127.83	4.34	14.096	27.644	BDL
KH18	n.a.	5.42	14.87	88.78	3.32	31.204	80.178	BDL
KH19	n.a.	1.74	6.77	76.86	2.36	9.85	23.022	BDL
KH20	n.a.	1.9	6.78	66.37	2.32	9.051	17.874	BDL
KH21	0.46	6.76	40.53	177.56	7.72	29.911	100.789	BDL
KH22	n.a.	3.47	9.5	82.98	2.97	10.167	29.707	BDL
KH23	n.a.	2.45	33.78	115.09	4.39	13.381	35.848	BDL
KH24	n.a.	5.02	7.07	84.24	2.59	8.594	20.93	BDL
KH25	n.a.	2.72	11.9	60.89	1.94	6.522	29.481	BDL
KH26	n.a.	3.56	8.8	144.13	4	13.833	21.219	BDL
KH27	1.02	15.22	66.78	171.72	8.29	37.333	70.978	BDL
BA20	1.07	4.27	30.31	142.57	5.47	19.504	35.87	BDL
BA21	1.21	4.26	28.76	133.33	5.29	19.293	36.904	BDL
BA22	0.56	4.25	41.56	172.32	6.89	27.248	55.756	BDL
BA23	0.59	4.33	28.64	150.37	5.38	18.567	56.93	BDL

Sample ID	Ammonium (mg/L)	Potassium (mg/L)	Magnesium (mg/L)	Calcium (mg/L)	Strontium (mg/L)	Li (µg/l)	B (µg/l)	P (µg/l)
BA24	1.37	5.51	32.04	145.77	5.43	26.241	64.604	BDL
BA25	0.44	4.8	24.79	105.21	3.77	13.696	53.141	BDL
BA26	n.a.	2.91	17.35	91.58	3.11	11.874	25.522	BDL
BA27	n.a.	1.98	5.99	58.62	1.68	6.849	17.704	BDL
BA28	n.a.	2.82	19.31	129.04	4.04	11.505	39.956	BDL
BA29	n.a.	2	5.63	62.62	1.75	7.068	14.93	BDL
BA30	n.a.	2.2	5.41	91.57	2.09	7.076	12.526	BDL
BA31	n.a.	3.25	6.93	144.47	3.55	9.347	16.504	BDL
BA32	n.a.	2.14	2.99	70.1035	1.88	6.537	14.174	BDL
BA33	0.13	3.28	29.26	152.5	5.96	15.637	46.293	BDL
BA34	1.67	6.96	43.81	207.52	7.99	31.807	66.385	BDL
BA35	2.22	3.49	12.46	102.94	3.34	14.396	18.915	BDL
BA36	0.23	3.34	24.12	125.99	4.44	13.322	40.63	BDL
10C	BDL	21.3	5.5	95	6.1	31.3	102.5	n.d.
21B	BDL	7.3	27.8	87.2	5.2	50.2	195.6	n.d.
26B	BDL	51.4	163.8	525.2	30.3	239.2	652.2	n.d.
29B	BDL	4.5	6.3	48.7	2.4	22.1	59.9	n.d.
35B	BDL	3.9	12.4	46.4		29.9	120.7	n.d.
42B	BDL	123.8	13.4	310.6	37.2	123.2	298.1	n.d.
50B	BDL	9	3.1	66.7		11.5	69.5	n.d.
6B	BDL	3.4	11.5	88.3	3.1	20.2	61.1	n.d.
BB5HA	BDL	14.9	4.2	82.5	5	29.2	77.7	n.d.
10D	BDL	8.3	4.4	78		20.2	54.9	n.d.
21C	BDL	1.8	21.2	239.2	10.4	21	55.5	n.d.
26C	BDL	2.6	3.8	14.1	1	20.6	106.6	n.d.
29C	BDL	1.9	3.4	32.8	1.4	8.2	39.5	n.d.
34B	BDL	1	4.7	43.3	1.9	6.8	57.4	n.d.
35C	BDL	1.7	6.8	89.5	3.7	9.8	39.3	n.d.
36D	BDL	3.9	8	88.1	4	23.3	67.8	n.d.
42C	BDL	7.6	3.2	62.3	3.2	12.6	66.3	n.d.
50C	BDL	3.9	15.8	127.4	5.7	17.6	64.4	n.d.
51B	BDL	4.3	3.3	54.6		17.1	66.9	n.d.
52B	BDL	4.5	3.5	61.3		15.6	59.7	n.d.
6C	BDL	3.5	11.4	86.9	3.3	18.1	63	n.d.
BB5HB DUP	BDL	4.8	3	53.5	2.6	13.7	48.2	n.d.
BB8	BDL	8.8	3.3	52.7	2.9	16.7	71.2	n.d.
BA FieldBlank	n.a.	n.a.	n.a.	n.a.	n.a.			

Sample ID	V (µg/l)	Cr (µg/l)	Mn (µg/l)	Fe (µg/l)	Co (µg/l)	Ni (µg/l)	Cu (µg/l)	Zn (µg/l)	As (µg/l)	Se (µg/l)	Mo (µg/l)	Cd (µg/l)	Hg (µg/l)
BA01	2	BDL	BDL	1	0.048	0.113	6	45	0.607	1.152	0.386	BDL	3.83
BA02	2	BDL	143	1	0.113	0.074	2	11	0.283	0.312	2.267	0.028	6.56
BA03	2	BDL	BDL	BDL	0.065	0.157	1	13	0.098	1.697	0.481	0.016	3.56
BA04	2	BDL	BDL	BDL	0.088	0.211	1	1	0.472	2.109	0.352	0.016	4.7
BA05	1	BDL	BDL	BDL	0.065	0.212	1	15	0.091	9.299	0.6	0.021	3.75
BA06	2	BDL	BDL	1	0.07	0.157	4	28	0.386	5.434	0.588	0.021	4.3
BA07	1	BDL	BDL	1	0.097	0.074	1	13	0.21	3.777	0.749	0.025	2.51
BA08	2	BDL	BDL	BDL	0.035	BDL	1	BDL	0.159	8.341	1.179	0.003	3.83
BA09	1	BDL	BDL	BDL	0.049	0.065	1	14	0.287	3.092	0.54	0.008	4.97
BA10	2	BDL	BDL	BDL	0.046	0.119	1	9	0.166	3.839	0.723	0.036	2.22
BA11	2	BDL	13	42	0.05	0.185	1	8	0.317	1.798	0.745	0.018	1.88
BA12	1	BDL	40	134	0.069	0.156	BDL	6	0.383	1.461	0.605	0.039	3.4
BA13	1	BDL	BDL	3	0.051	0.126	3	15	0.186	2.954	1.015	0.02	2.39
BA14	2	BDL	BDL	BDL	0.059	0.076	1	8	0.617	2.927	0.896	0.018	6.8
BA15	4	BDL	BDL	BDL	0.04	0.109	2	1	0.668	3.255	0.956	BDL	4.35
BA16	1	BDL	24	BDL	0.065	0.079	4	BDL	0.417	2.546	1.214	0.015	5.65
BA17	1	BDL	103	1	0.079	0.074	4	BDL	1.075	0.695	1.385	0.033	4.63
BA18	2	BDL	101	BDL	0.197	0.28	4	10	0.776	21.137	0.998	0.024	5.02
BA19	2	BDL	BDL	2	0.086	0.159	6	21	0.202	27.315	0.417	0.061	4.76
KH01	3	BDL	BDL	2	0.077	0.42	1	13	0.939	1.397	0.592	0.024	37.76
KH02	BDL	BDL	BDL	BDL	BDL	BDL	BDL	BDL	BDL	BDL	0.006	BDL	11.55
KH03	3	BDL	BDL	BDL	0.067	0.706	2	10	0.509	1.979	0.485	0.143	6.47
KH04	1	BDL	1	4	0.055	0.196	1	2	0.291	1.305	0.628	0.031	56.33
KH05	3	BDL	1	2	0.054	0.468	3	9	0.172	0.576	0.56	0.048	37.44
KH06	1	BDL	1	1	0.132	2.239	7	14	0.183	1.471	0.375	0.124	18.34
KH07	4	BDL	BDL	BDL	0.044	0.113	1	9	1.822	0.708	0.248	0.013	18.33
KH08	1	BDL	1	BDL	0.057	0.159	2	27	0.188	1.494	0.254	0.058	21.55
KH09	1	BDL	BDL	4	0.062	0.134	1	13	0.38	1.381	0.254	0.03	20.15
KH10	3	BDL	11	1	0.311	1.007	2	7	1.178	3.301	0.781	0.05	14.13
KH11	2	BDL	BDL	BDL	0.196	0.988	3	11	0.849	2.479	0.666	0.122	14.79
KH12	1	BDL	BDL	3	0.069	0.208	4	9	0.287	1.527	0.358	0.022	13.54
KH13	1	BDL	BDL	BDL	0.046	0.722	58	37	0.145	2.909	0.483	0.156	8.11
KH14	3	BDL	BDL	BDL	0.064	0.358	1	10	0.704	0.527	0.655	0.038	8.91
KH15	6	BDL	11	6	0.147	0.456	4	17	1.009	1.756	0.075	0.017	16.65
KH16	5	BDL	BDL	4	0.057	0.062	5	BDL	0.59	0.449	0.331	BDL	8.19
KH17	1	BDL	BDL	3	0.094	0.3	BDL	BDL	0.44	1.297	0.353	BDL	9.16
KH18	3	BDL	3	4	0.059	0.128	BDL	1	0.677	1.001	1.64	BDL	25.5
KH19	3	2	BDL	2	0.043	BDL	BDL	8	0.398	0.506	0.282	BDL	7
KH20	5	1	BDL	1	0.042	BDL	1	1	1.176	0.351	0.139	BDL	4.06
KH21	1	BDL	BDL	4	0.219	0.905	1	8	0.457	3.966	0.718	0.021	11.9
KH22	1	BDL	BDL	2	0.039	0.087	2	16	0.359	1.014	0.314	BDL	8.71
KH23	1	6	1	18	0.117	3.235	8	BDL	0.374	15.163	0.616	BDL	5.4
KH24	1	BDL	BDL	3	0.05	0.095	1	13	0.091	2.696	0.327	BDL	4.57
KH25	1	BDL	BDL	1	0.051	0.135	2	8	0.158	0.208	0.044	0.016	5.01
KH26	5	2	BDL	BDL	0.073	0.166	7	BDL	1.284	4.553	0.081	BDL	7.36
KH27	1	BDL	1	11	0.211	1.179	112	10	0.24	4.631	0.576	0.032	7.14
BA20	1	BDL	BDL	3	0.078	0.189	4	4	0.32	2.741	1.088	0.04	8.67
BA21	1	BDL	1	7	0.081	0.151	4	1	0.39	2.831	1.556	0.024	7.85
BA22	1	BDL	BDL	3	0.14	0.525	7	62	0.225	3.469	1.188	0.178	7.03
BA23	1	BDL	BDL	4	0.103	0.221	4	BDL	0.184	2.181	0.849	BDL	6.93

Sample ID	V (µg/l)	Cr (µg/l)	Mn (µg/l)	Fe (µg/l)	Co (µg/l)	Ni (µg/l)	Cu (µg/l)	Zn (µg/l)	As (µg/l)	Se (µg/l)	Mo (µg/l)	Cd (µg/l)	Hg (µg/l)
BA24	1	BDL	BDL	2	0.111	0.366	4	7	0.403	3.324	0.516	0.02	8.2
BA25	1	BDL	1	14	0.082	0.208	6	36	0.253	1.045	1.244	BDL	5.49
BA26	1	BDL	BDL	1	0.049	0.254	7	2	0.337	1.15	0.614	0.021	3.62
BA27	2	BDL	BDL	1	0.036	BDL	9	8	0.666	0.317	0.333	0.022	2.49
BA28	1	BDL	BDL	1	0.088	0.269	8	5	0.206	1.535	0.601	0.033	3.61
BA29	4	BDL	BDL	3	0.031	BDL	4	BDL	1.157	0.173	0.114	BDL	3.69
BA30	4	1	BDL	1	0.049	0.068	4	3	0.816	0.327	0.06	0.014	1.82
BA31	2	BDL	BDL	1	0.077	0.161	8	14	0.521	0.552	0.116	0.02	3.51
BA32	5	BDL	BDL	1	0.064	0.093	5	16	0.184	0.227	0.236	0.068	1.23
BA33	2	BDL	BDL	1	0.091	0.264	10	9	0.179	1.933	0.786	0.052	3.84
BA34	1	BDL	BDL	BDL	0.118	0.316	11	BDL	0.4	5.569	0.639	0.025	5.81
BA35	1	BDL	77	3	0.183	0.228	4	4	0.566	0.151	0.559	0.036	6.19
BA36	1	BDL	BDL	2	0.071	0.156	4	8	0.278	1.96	0.858	0.081	3.4
10C	1.6	0.2	158.2	8.6	0	1.7	12.2	34.6	3.3	BDL	9.4	0.3	n.d.
21B	5.8	3.9	3.2	92.3	0.4	18.8	10.1	4.9	1.9	4.5	8.1	0.2	n.d.
26B	1.4	0.7	131.8	29.7	0.1	1.4	6.6	BDL	0.9	2.7	3.1	0.4	n.d.
29B	10.7	8.1	1	2.6	0.1	0.6	6.9	4.8	1.5	2.5	2.9	0.1	n.d.
35B	8.1	1.5	1.3	15.1	BDL	1.6	5.6	34.1	1.8	3.1	2.5	0.2	n.d.
42B	0.8	1.3	169.4	622.9	0.6	2.2	8.2	BDL	3.1	0.6	9.4	0.2	n.d.
50B	0.3	0.1	132.6	1	0	2.1	8.6	17.2	9.6	BDL	8.4	0.1	n.d.
6B	3.2	1	1.7	2.8	0.2	1.9	5	31.2	0.7	3.3	4.5	0.2	n.d.
BB5HA	1	1.5	947.1	55.6	0.3	5.7	7.2	59.2	0.9	BDL	16.5	0.3	n.d.
10D	0.9	0.2	13.6	147.4	0	0.8	7.6	6.7	0.3	0.8	4	0.2	n.d.
21C	7.1	0.4	1.5	9.4	BDL	4.1	11.3	13.6	1.3	0	0.5	0.2	n.d.
26C	16.4	1.4	1.3	8.1	BDL	1.7	6.3	BDL	2.2	2.4	6	0.2	n.d.
29C	6.2	0.7	1.1	6.2	BDL	1.2	4.5	22.4	1.8	0.5	0.7	0.2	n.d.
34B	8.6	0.7	1.7	4.4	BDL	0.8	4.5	52.1	1.9	2.2	0.5	0.3	n.d.
35C	6.6	0.4	0.8	2.4	BDL	1.1	4.9	16.9	1.3	0.1	0.5	0.1	n.d.
36D	8.6	1.1	1.2		BDL	1.4	4.8	45.3	2.3	3.9	2.4	0.3	n.d.
42C	4.7	0.9	3.9	0.5	BDL	0.8	7.8	5.2	1.4	1.7	2.1	0.2	n.d.
50C	3.4	4	2.2	4.7	1.3	4.1	7.5	25.6	0.5	1.1	4	0.4	n.d.
51B	1.3	0.2	1.1		BDL	0.6	5.3	25.8	0.3	10.6	3.7	0.2	n.d.
52B	2.4	1.2	3.3	22.2	BDL	3.2	6.7	40.4	0.9	2.5	6	0.1	n.d.
6C	3.2	0.9	1.4	1.1	BDL	0.7	4.4	12.4	0.5	1.4	3.2	0.2	n.d.
BB5HB DUP	2.8	0.8	32	23.7	BDL	0.8	7.4	31.8	2.1	0.5	4.4	0.3	n.d.
BB8	1.6	0.7	11	27.7	BDL	2.2	9	6	0.7	7.3	3.3	0.1	n.d.
BA_FieldBlank													

Sample ID	U (µg/l)	Charge imbalance Error	NPOC (mg/L)	TN (mg/L)	Well depth (ft)	Screen depth (ft)
BA01	1.42	-4.89%	0.7427	2.674	110	n.d.
BA02	3.12	-2.41%	0.6397	0.206	175	n.d.
BA03	4.02	-0.87%	1.399	4.215	70	50-70
BA04	3.76	-2.93%	1.952	6.373	80	60-80
BA05	8.1	-2.65%	1.153	10.42	50	35-50
BA06	6.51	-1.65%	1.155	15.47	65	n.d.
BA07	2.09	-2.31%	0.8946	10.02	76	56-76
BA08	2.7	1.99%	0.6603	3.997	68	48-68
BA09	1.95	-1.75%	1.009	2.099	90	50-62
BA10	1.83	-1.09%	1.067	5.835	67	n.d.
BA11	1.17	-0.12%	1.002	5.497	80	n.d.
BA12	2.44	-1.21%	1.002	2.568	66	n.d.
BA13	1.31	-5.57%	1.044	6.075	60	n.d.
BA14	8.51	2.87%	1.193	19.84	67	n.d.
BA15	3	0.47%	1.852	5.534	65	45-65
BA16	4.48	-6.70%	1.006	2.517	85	n.d.
BA17	3.29	-3.68%	1.284	0.2141	110	n.d.
BA18	3.22	-1.67%	0.9664	2.221	50	30-50
BA19	3.57	-1.22%	1.256	11.26	n.d.	n.d.
KH01	3.36	-0.15%	1.235	7.393	57	47-57
KH02	1.18	5.90%	1.155	0.4387	78	58-78
KH03	5.98	0.29%	2.189	18.26	n.d.	n.d.
KH04	3.16	-3.30%	1.207	3.541	63	43-63
KH05	1.27	0.61%	2.257	3.301	68	48-68
KH06	4.81	-4.53%	2.497	41.82	62	42-62
KH07	0.94	4.38%	1.546	11.59	100	n.d.
KH08	1.45	4.64%	1.469	12.04	101	n.d.
KH09	1.57	4.74%	1.083	9.56	80	n.d.
KH10	8.61	-1.42%	1.784	4.501	65	55-65
KH11	2.67	1.09%	2.112	7.127	50	30-50
KH12	2.23	2.95%	1.231	14.81	n.d.	n.d.
KH13	1.73	-2.86%	3.282	5.253	n.d.	n.d.
KH14	2.97	2.50%	1.846	27.36	60	n.d.
KH15	1.74	-5.49%	n.d.	n.d.	60	40-60
KH16	1.47	-2.12%	n.d.	n.d.	92	72-92
KH17	2.21	-5.03%	n.d.	n.d.	110	75-110
KH18	1.42	-5.99%	n.d.	n.d.	44	n.d.
KH19	1.06	-0.60%	n.d.	n.d.	123	n.d.
KH20	0.87	-5.77%	n.d.	n.d.	n.d.	n.d.
KH21	9.72	-0.31%	n.d.	n.d.	n.d.	n.d.
KH22	1.39	-1.09%	n.d.	n.d.	n.d.	n.d.
KH23	5.88	1.85%	n.d.	n.d.	n.d.	n.d.
KH24	3.48	-2.85%	n.d.	n.d.	76	n.d.
KH25	0.43	-0.50%	n.d.	n.d.	n.d.	n.d.
KH26	1.09	n.d.	n.d.	n.d.	61	41-61
KH27	9.32	1.98%	n.d.	n.d.	40	20-40
BA20	10.94	3.38%	0.7179	7.549	52	42-52
BA21	10.4	1.15%	0.8677	7.388	50	40-50
BA22	14.31	0.40%	1.181	28.38	n.d.	n.d.
BA23	11.24	0.12%	0.8942	16.92	31	n.d.

Sample ID	U (µg/l)	Charge imbalance Error	NPOC (mg/L)	TN (mg/L)	Well depth (ft)	Screen depth (ft)
BA24	11.43	1.32%	0.9979	10.04	n.d.	n.d.
BA25	10.03	0.55%	1.262	23	78	58-78
BA26	4.43	0.40%	0.664	11.51	54	26-54
BA27	0.3	-1.36%	0.5666	8.912	n.d.	n.d.
BA28	5.43	-0.35%	1.009	16.75	53	43-53
BA29	0.29	2.50%	0.4335	1.152	n.d.	n.d.
BA30	1.91	0.91%	0.7792	8.207	81	69-81
BA31	1.64	-0.40%	1.176	15.81	91	n.d.
BA32	0.84	-1.01%	0.5833	5.829	60	45-60
BA33	10.24	-2.89%	1.09	21.78	60	40-60
BA34	9.89	0.87%	1.399	13.63	105	90-105
BA35	1.99	2.48%	0.9377	0.131	26	n.d.
BA36	6.24	1.32%	1.011	13.99	49	39-49
10C	1.4	-2.80%	n.d.	n.d.	105	100-105
21B	1.6	-4.30%	n.d.	n.d.	118	n.d.
26B	4.2	-2.00%	n.d.	n.d.	123	118-123
29B	1.7	-2.50%	n.d.	n.d.	125	120-125
35B	1.8	-3.30%	n.d.	n.d.	155	150-155
42B	1.9	-4.10%	n.d.	n.d.	162	157-162
50B	0.7	-2.10%	n.d.	n.d.	130	125-130
6B	2.8	-3.20%	n.d.	n.d.	146	135-145
BB5HA	1.7	-2.00%	n.d.	n.d.	140	120-140
10D	61.2	-6.50%	n.d.	n.d.	79	73-79
21C	2.7	-9.20%	n.d.	n.d.	48	43-45
26C	1.5	-1.30%	n.d.	n.d.	65	60-65
29C	0.2	-7.20%	n.d.	n.d.	65	62-65
34B	0.9	-9.20%	n.d.	n.d.	34	29-34
35C	1.4	-8.50%	n.d.	n.d.	71	66-71
36D	3	-6.30%	n.d.	n.d.	90	85-90
42C	1	-7.90%	n.d.	n.d.	108	103-108
50C	4.5	-6.50%	n.d.	n.d.	50	45-50
51B	1.9	-2.60%	n.d.	n.d.	100	95-100
52B	3.7	-4.50%	n.d.	n.d.	102	97-102
6C	3.3	-2.90%	n.d.	n.d.	70	60-70
BB5HB DUP	1	-4.70%	n.d.	n.d.	75	65-75
BB8	2.8	-5.50%	n.d.	n.d.	150	130-150
BA_FieldBlank		-100%				

	Clay above the screen				
Sample ID	(ft)				
BA01	n.d.				
BA02	n.d.			n.d.	no data
BA03	14			BDL	below detection limit
BA04	33			n.a.	not applicable
BA05	28				
BA06	n.d.				
BA07	45				
BA08	n.d.				
BA09	n.d.				
BA10	n.d.				
BA11	n.d.				
BA12	n.d.				
BA13	n.d.				
BA14	n.d.				
BA15	20				
BA16	n.d.				
BA17	n.d.				
BA18	26				
BA19	n.d.				
KH01	2				
KH02	30				
KH03	n.d.				
KH04	38				
KH05	40				
KH06	35				
KH07	n.d.				
KH08	n.d.				
KH09	n.d.				
KH10	30				
KH11	25				
KH12	n.d.				
KH13	n.d.				
KH14	n.d.				
KH15	8				
KH16	45				
KH17	55				
KH18	n.d.				
KH19	n.d.				
KH20	n.d.				
KH21	n.d.				
KH22	n.d.				
KH23	n.d.				
KH24	n.d.				
KH25	n.d.				
KH26	41				
KH27	8				
BA20	n.d.				
BA21	n.d.				
BA22	n.d.				
BA23	n.d.				

Sample ID	Clay above the screen (ft)				
BA24	n.d.				
BA25	n.d.				
BA26	n.d.				
BA27	n.d.				
BA28	n.d.				
BA29	n.d.				
BA30	n.d.				
BA31	n.d.				
BA32	n.d.				
BA33	n.d.				
BA34	n.d.				
BA35	n.d.				
BA36	n.d.				
10C	39				
21B	n.d.				
26B	40				
29B	22				
35B	21				
42B	67				
50B	16				
6B	n.d.				
BB5HA	26				
10D	22				
21C	5				
26C	34				
29C	3				
34B	19				
35C	8				
36D	11				
42C	28				
50C	15				
51B	13				
52B	44				
6C	n.d.				
BB5HB DUP	8				
BB8	66				
BA_FieldBlank					

*** n.d. = No Data

***BDL = Below Detection Limit

***n.a. = Not Applicable (not measured)

Detection limits for anions and cations, measured on an Ion Chromatograph ICS-1100. Detection limits for trace elements, measured on an Inductively Coupled Plasma Mass Spectrometer ICP-MS.

Anion	Fluoride	Chloride	Nitrite	Bromide	Nitrate	Sulfate
Units	mg/L	mg/L	mg/L	mg/L	mg/L	mg/L
Detection Limit	0.08	0.68	0.71	0.058	0.59	0.81

Cation	Sodium	Ammonium	Potassium	Magnesium	Calcium	Strontium
Units	mg/L	mg/L	mg/L	mg/L	mg/L	mg/L
Detection Limit	1.51	0.24	0.44	0.4	0.41	0.53

Trace Element	Lithium / 7	Boron / 11	Phosphorous / 31	Vanadium / 51	Chromium / 52	Manganese / 55
Units	(µg/l)	(µg/l)	(µg/l)	(µg/l)	(µg/l)	(µg/l)
Detection Limit	0.044	0.00001	10	0.16	0.09	0.02

Trace Element	Iron / 56	Cobalt / 59	Nickel / 60	Copper / 63	Zinc / 66	Arsenic / 75
Units	(µg/l)	(µg/l)	(µg/l)	(µg/l)	(µg/l)	(µg/l)
Detection Limit	0.33	0.01267	0.059	0.1	0.19	0.033

Trace Element	Selenium / 78	Molybdenum / 95	Cadmium / 111	Mercury / 201	Uranium / 238
Units	(µg/l)	(µg/l)	(µg/l)	(µg/l)	(µg/l)
Detection Limit	0.038	0.018	0.01278	0.04	0

Appendix B - Land Use/Land Cover Descriptions

The Kansas Land Cover 2015 L1 map has 10 LULC descriptions, Commercial/Industrial (11), Urban Residential (12), Urban Openland (13), Urban Woodland (14), Urban Water (15), Cropland (20), Grassland (30), Woodland (40), Water (50), Other (60) (KBS, 2015).
The Commercial/Industrial (11) class is land that is used heavily and covered by buildings or other hard surfaces, some specific examples include central business districts, roads and highways, parking lots and structures, and landscaped areas (KARS, 2015). The Urban Residential (12) class is characterized by an even distribution of flora and fauna, and it includes houses, apartment complexes, surrounding streets, driveways, garages, and parking areas (KARS, 2015). The Urban Openland (13) class includes golf courses, cemeteries, undeveloped land within urban areas, parks, and zoos (KARS, 2015).

The Urban Woodland (14) class includes wooded areas in urban settings. Urban Water (15) consists of any water surfaces within cities or towns, specific examples include lakes and sewage ponds (KARS, 2015). Cropland (20) consists of any active agricultural land, as well as uniform plots of bare land, and plowed/mowed land (KARS, 2015). The Grassland (30) classification includes grass land, range land, and hayed land (KARS, 2015). Woodland (40) areas have a canopy density of 50% or greater (KARS, 2015). The Water (50) classification includes bodies of surface water, not in urban regions (KARS, 2015). The Other (60) classification includes undefined areas such as gravel pits, rock quarries, and sand bars (KARS, 2015). Our data set did not include any Other (60) classification.

Appendix C - Groundwater Quality Report Example

Well ID	Date	Time	Land use	Latitude	Long	pH	T (c)	Cond (µS)	DO mg/L	DO% sat
BA_01	6/11/2021	11:30 AM	Irrigated crop	x	x	7.47	18.9	598.3	4.6	56
T (c)	Cond.	Specific	Alkalinity	CaCO3	Fluoride	Chloride	Nitrite	Bromide	Nitrate	N
DO probe	µS/cm	µS/cm	meq/L	as mg/L	mg/L	mg/L	mg/L	mg/L	mg/L	mg/l as N
18.8	658	713	3.81	190.9	0.3193	30.2205	n.a.	0.0647	115.416	26.076087
					4 mg/L	250 mg/L	1 mg/L			10 mg/L
Phosphate	Sulfate	Sodium	Ammonium	Potassium	Magnesium	Calcium	Strontium	Li	B	P
mg/L	mg/L	mg/L	mg/L	mg/L	mg/L	mg/L	mg/L	ppt	ppt	ppm
n.a.	23.651	32.9178	n.a.	3.3767	11.0595	79.9575	2.4079	8758	25219	2
	250 mg/L									
V	Cr	Mn	Fe	Co	Ni	Cu	Zn	As	Se	Mo
ppb	ppb	ppb	ppb	ppt	ppt	ppb	ppb	ppt	ppt	ppt
2	0	0	1	48	113	6	45	607	1152	386
	100 ppb	500 ppb	300 ppb			1300 ppb	5000 ppb	10,000 ppt	50,000 ppt	
Cd	Hg	U								
ppt	ppb	ppb				Exceeds secondary standard				
7	3.83	1.42				**Exceeds primary standard**				
5000 ppt	2 ppb	30 ppb				**Maximum Contaminant Level (EPA)**				
						ppt = parts per thousand (ng/L)				
Charge imbalance	NPOC	Total Nitrogen	Well depth			ppb = parts per billion (µg/L)				
meq/l	mg/L	mg/L	ft			ppm = parts per million (mg/L)				
-4.89%	0.7427	2.674	110							